



Solid lipid nanoparticles cyclodextrin-decorated incorporated into gellan gum-based dry floating in situ delivery systems for controlled release of bioactive compounds of safflower (*Carthamus tinctorius*. L): A proof of concept study in biorelevant media

Andi Dian Permana^{a,*}, Anwar Sam^a, Ardiyah Nurul Fitri Marzaman^a, Abdul Rahim^a, Firzan Nainu^a, Muh. Akbar Bahar^a, Rangga Meidianto Asri^a, Lutfi Chabib^b

^a Faculty of Pharmacy, Hasanuddin University, Makassar 90245, Indonesia

^b Department of Pharmacy, Universitas Islam Indonesia, Yogyakarta 55584, Indonesia

ARTICLE INFO

Keywords:

Safflower
Solid lipid nanoparticles
Floating gel in situ

ABSTRACT

Safflower (*Carthamus tinctorius* L.) has been explored as a source of natural antioxidant. However, quercetin 7-O-beta-D-glucopyranoside and luteolin 7-O-beta-D-glucopyranoside, as its bioactive compounds, possessed poor aqueous solubility, limiting its efficacy. Here, we developed solid lipid nanoparticles (SLNs) decorated with hydroxypropyl beta-cyclodextrin (HPβCD) incorporated into dry floating gel in situ systems to control the release of both compounds. Using Geleol® as a lipid matrix, SLNs were <200 nm in size with >80 % of encapsulation efficiency. Importantly, following the decoration using HPβCD, the stability of SLNs in gastric environment was significantly improved. Furthermore, the solubility of both compounds was also enhanced. The incorporation of SLNs into gellan gum-based floating gel in situ provided desired flow and floating properties, with <30 s gelation time. The floating gel in situ system could control the release of bioactive compounds in FaSSGF (Fasted-State Simulated Gastric Fluid). Furthermore, to assess the effect of food intake on release behavior, we found that the formulation could show a sustained release pattern in FeSSGF (Fed-State Simulated Gastric Fluid) for 24 h after being released in FaSSGF for 2 h. This indicated that this combination approach could be a promising oral delivery for bioactive compounds in safflower.

1. Introduction

Recently, oxidative stress, caused by free radicals, has been reported to be the main foremost reason for numerous chronic diseases [1,2], including autoimmune diseases [3], chronic kidney disease [4], neurodegenerative diseases [5], cardiovascular diseases [6], cancer [7] and liver diseases [8]. Normally, as free radical, reactive oxygen species (ROS) are regularly generated in human cells. To neutralize the undesired effects of ROS, cells continuously produce endogen antioxidant systems consisting of enzymes and non-enzymatic compounds [9,10]. These endogen antioxidants are able to inhibit the reaction of ROS. Nevertheless, in some disease conditions, there is a decrease in the generation of endogen antioxidants, resulting in the increment of the ratio of antioxidant and ROS [11]. Despite the fact that the synthetic antioxidants have been extensively explored, the natural antioxidants

from plants, vegetables, and fruits have been found to be a significant resource of antioxidants [12]. Accordingly, a plethora of studies have investigated different sources of natural plants for their potential as antioxidant agents [13–15]. The main reason for this was mainly due to several advantages of natural antioxidants over synthetic antioxidants, namely less adverse effects and fewer economic costs.

Safflower (*Carthamus tinctorius*. L), belonging to from Asteraceae family, has been widely explored for its antioxidant compounds. Safflower is mainly cultivated exclusively for its flowers, which are applied in the therapy of several diseases. The antioxidant properties of safflower are mainly due to several compounds, namely flavonoid and phenolic compounds [16–18]. Specifically, the glycosides form of the flavonoid compounds in safflower, namely quercetin 7-O-beta-D-glucopyranoside and luteolin 7-O-beta-D-glucopyranoside have been found to possess strong antioxidant properties which can potentially protect the

* Corresponding author at: Department of Pharmaceutical Science and Technology, Faculty of Pharmacy, Hasanuddin University, Indonesia.

E-mail address: andi.dian.permana@farmasi.unhas.ac.id (A.D. Permana).

body from stress oxidative [16,19,20]. However, although those compounds possess adequate antioxidant activities, they have poor aqueous solubility, limiting their bioavailability and efficacy as antioxidant in the human body. Accordingly, there is a necessity to develop a delivery system to improve the solubility of these compounds.

Among several delivery systems, the interest of researchers in solid lipid nanoparticles (SLNs) has increased significantly. This system has shown significant benefits, namely high entrapment efficiency, enhancement of solubility profiles and control release manner in comparison with other lipid-based delivery system [21]. SLNs are consisted of physiological lipids, making this system to be considered safe for the administration. Importantly, SLNs have been extensively applied to enhance the solubility and control the release of numerous hydrophobic compounds [22–24]. With respect to the administration route, the oral route has been considered the most convenient and acceptable route for drug administration [25]. However, the poor stability and high propensity to aggregate in acid conditions limited their application through the oral route [26]. Several studies have shown that the oral administration of SLNs could result in instability of the particles in the gastric environment [27,28]. Accordingly, it is crucial to investigate suitable approach to protect the SLNs from the gastric environment during oral administration. Previously, hydroxypropyl beta-cyclodextrin (HP β CD) has been found to improve the stability of SLNs administered orally [29]. The decoration of SLNs containing amphotericin B, paramomycin and paclitaxel using HP β CD could improve their efficacies for their respective pharmacological effects [29,30]. Therefore, the incorporation of bioactive compounds of safflower into SLNs decorated with HP β CD could be an appropriate strategy for improved solubility.

To facilitate the oral administration of the SLNs, it was important to develop a suitable system. One of delivery systems to control and sustain the release of drugs through oral administration is gastroretentive drug delivery system (GRDDS). In this formulation, 100 % of drugs would stay in the stomach for a long period [31–33]. As one of GRDDS, in situ forming gel system has attracted the interest in drug delivery due to the transformation of the formulation from solution into a floating gel when administered orally and reaching the gastric environment [34–36]. Numerous studies have explored the effectiveness of this system to control the release some drugs administered orally [32,37,38]. As one of macromolecules compounds, gellan gum has been widely used to develop GRDDS preparations, showing the controlled release pattern of the bioactive compounds [32,39–41].

In this study, we extracted the bioactive compounds from safflower and formulated the extract into SLNs. The SLNs were decorated using HP β CD to improve its gastric stability. Several characterizations were carried out to optimize the SLNs. Afterwards, the SLNs were further incorporated into floating gel in situ system using gellan-gum as a main matrix molecule in the dry form which would be dispersed in water prior to the oral administration. The floating gel in situ was evaluated for their properties and release behavior of quercetin 7-O-beta-D-glucopyranoside and luteolin 7-O-beta-D-glucopyranoside as the interest compounds. The effect of food intake on the dissolution profile was further investigated as a proof of concept study in biorelevant media. The main finding of this investigation showed the potential of using natural product as antioxidant sources in sustain release formulation for potential treatment of oxidative stress induced diseases.

2. Materials and methods

2.1. Materials

The safflower samples were collected from Bone, South Sulawesi, Indonesia. Geleol® was kindly gifted by Gattefosse Pvt. Ltd., France. Hydroxypropyl beta-cyclodextrin was kindly gifted by Cyclolab Ltd., Budapest, Hungary. Gellan gum, sodium citrate, calcium chloride, poly (vinyl alcohol) PVA (9–10 kDa), Tween80 and sodium dihydrogen phosphate were obtained from Sigma-Aldrich (Dorset, UK). Other

chemicals utilized in this study were analytical grade and applied without purification process.

2.2. Extraction of safflower

The safflower flowers were dried and grounded. Afterward, the samples (500 g) were extracted using three different solvents, namely absolute ethanol (Et100), 75 % ethanol (Et75), 50 % ethanol (Et50), 25 % ethanol (Et25) and water (Wat). Percolation method was used to extract the bioactive compounds at room temperature [42]. The mixtures were then filtered, and the filtrate was subjected to a rotary evaporator (Büchi Rotavapor R-114, Büchi, Switzerland) and freeze drying (Christ, Osterode am Harz, Germany), obtaining a dry extract of Et100, Et75, Et50, Et25 and Wat.

2.3. Determination of extraction yields of safflower

The yield of the extraction process using different solvents was calculated using the following equation [43]:

$$\text{Extraction yield (\%)} = \frac{\text{Mass of dried extract}}{\text{Mass of initial samples}} \times 100\%$$

2.4. Determination of total flavonoid and phenolic contents

The total flavonoid content (TFC) of safflower extract was measured by colorimetry utilizing AlCl₃ [43], with minor modification. Briefly, the methanolic solution of safflower extract was mixed with 10 % w/v AlCl₃ (0.25 mL) and potassium acetate solution (0.5 mL). The solution was incubated for 25 min in the dark. The absorbance of the solution was detected using a spectrophotometer (Shimadzu, Kyoto, Japan) at 415 nm. Quercetin was used as a standard compound. The amount of TFC was reported as milligrams of quercetin equivalent per gram of extract (mg Qu/g).

The determination of total phenolic content (TPC) of safflower extract was carried out utilizing the Folin-Ciocalteu method [43], with a slight modification. The extract was initially solubilized in methanol. Afterwards, 250 μ L of the extract solution was mixed with 1 N Folin-Ciocalteu reagent (0.5 mL) and distilled water (5 mL). The solution was incubated for 10 min at room temperature, followed by the addition of 5 % w/v sodium carbonate solution (0.5 mL) and methanol (up to 10 mL) in the volumetric flask. The solution was incubated at room temperature for 25 min in dark condition. Finally, the absorbance of the solution was detected using a spectrophotometer at a wavelength of 760 nm. Gallic acid was used as the standard compound. The concentration of TPC was reported as milligrams of gallic acid equivalent per gram of extract (mg GAE/g).

2.5. Evaluation of antioxidant activity assay using DPPH scavenging capacity

The antioxidant properties of various extracts were evaluated using 2,2-diphenyl-1-picrylhydrazyl (DPPH) radical [43]. Briefly, the mixture of methanolic solution of DPPH (2.5 mL), methanolic solution of extract in various concentrations (0.25 mL) and methanol (2.5 mL) was incubated for 25 min in the dark at room temperature. The absorbance of the solution was detected using a spectrophotometer at 520 nm. The absorbance of the DPPH solution with the absence of extract solution was used as a control. The extraction solvents were utilized as blank. The antioxidant properties were determined using the following calculation:

$$\% \text{Inhibition} = \frac{\text{Absorbance of control} - \text{Absorbance of samples}}{\text{Absorbance of samples}} \times 100\%$$

Moreover, the concentration inhibiting 50 % of DPPH free radical (IC₅₀) was determined using linear regression in GraphPad Prism® version 6 (GraphPad Software, San Diego, California, USA).

Table 1
Condition of gradient analysis of HPLC method.

Time	TFA in water	Acetonitrile	Flow (mL/min)
0	90	10	0.5
3	70	30	0.5
6	40	60	0.6
9	30	70	0.6
12	75	25	0.5
15	90	10	0.5

Table 2
The formulation parameters of SLNs.

	Geleol	Extract	Tween	PVA	Sonication time
F1	100	100	1 %	–	5 min
F2	150	100	1 %	–	5 min
F3	200	100	1 %	–	5 min
F4	250	100	1 %	–	5 min
F5	100	100	–	1 %	5 min
F6	150	100	–	1 %	5 min
F7	200	100	–	1 %	5 min
F8	250	100	–	1 %	5 min
F9	100	100	1 %	–	10 min
F10	150	100	1 %	–	10 min
F11	200	100	1 %	–	10 min
F12	250	100	1 %	–	10 min
F13	100	100	–	1 %	10 min
F14	150	100	–	1 %	10 min
F15	200	100	–	1 %	10 min
F16	250	100	–	1 %	10 min

2.6. Evaluation of antioxidant activity using lipid peroxidation method

The lipid peroxidation antioxidant properties of the extract were assessed using thiocyanate, with slight modification [43]. Initially, linoleic acid (0.25 g), Tween-80 (0.25 g), and 20 mM phosphate buffer pH 7.0 (20 mL) were used to prepare linoleic emulsion. All compositions were mixed using an Ultra-Turrax® homogeniser (IKA, model T25, impeller 10 G, Germany). To perform the evaluation, the emulsion (2.5 mL) was mixed with methanolic solution of extract in various concentration levels. The mixture was incubated at 37 °C for 6 h. Afterward, the mixture (0.1 mL) was mixed with 75 % ethanol (5 mL), 20 mM of ferrous chloride in 100 mM HCl (0.1 mL) and 30 % w/v ammonium thiocyanate (0.2 mL). Then, the mixture was incubated at room temperature for 5 min. The absorbance of the solution was detected using a spectrophotometer at 500 nm. As per control, the absorbance of the mixture without the addition of extract was measured. The lipid peroxidation inhibition percentage was determined using the following calculation:

$$\% \text{Inhibition} = 100 - \frac{\text{Absorbance of samples}}{\text{Absorbance of control}} \times 100\%$$

Similarly, the concentration inhibiting 50 % of lipid peroxidation (IC50) was determined using linear regression in GraphPad Prism® version 6 (GraphPad Software, San Diego, California, USA).

2.7. HPLC assay of bioactive compounds in safflower extract

$$\text{Encapsulation efficiency (\%)} = \frac{\text{Compounds in formulation} - \text{unencapsulated compound}}{\text{Compounds in formulation}} \times 100\%$$

The quantification of bioactive compounds of safflower extract was performed using reverse phase HPLC (Shimadzu Prominence, Shimadzu, Kyoto, Japan). The gradient method (Table 1) using the mixture of 0.1 %

v/v trifluoro acetic acid (TFA) in water and acetonitrile was used to separate the compounds with a reversed-phase column C18 (150 × 4.6 mm, 5 μm) (Phenomenex, Inc., CA, USA). The samples were analyzed at 255 nm with injection volume of 25 μL. All the analysis process were carried at 25 °C. Quercetin 7-O-beta-D-glucopyranoside and Luteolin 7-O-beta-D-glucopyranoside were used as analytes of interest of the extract. The chromatogram analysis was carried out using Shimadzu LC solution software (ver. 1.21 SP1). The HPLC method applied to analyze both compounds was validated according to the International Committee on Harmonisation (ICH) 2005. The limit of detections of quercetin 7-O-beta-D-glucopyranoside and luteolin 7-O-beta-D-glucopyranoside were 0.15 μg/mL and 0.21 μg/mL with limit of quantifications of 0.35 μg/mL and 0.44 μg/mL, respectively. Importantly, the method was found to be precise and selective following inter-day and intraday measurements with R values > 0.999.

2.8. Solid lipid nanoparticles (SLNs) formulation

The SLNs were prepared using the emulsion-solvent evaporation technique [29]. The composition of the formulation is depicted in Table 2. Briefly, Geleol and extract were dissolved in 5 mL of mixture of chloroform and methanol (1:1). The organic phase was emulsified into 15 mL of stabilizer solutions under probe sonication (an amplitude of 75 % with 20 s pulse on and 10 s pulse off).

To modify the surface of SLNs using HPβCD, the SLNs dispersion was mixed with the same volume of HPβ-CD solution 1 % for 4 h at 100 rpm at 4 °C. In order to concentrate the SLNs and remove free compounds, the dispersion was spun for 30 min at 7500 rpm at 4 °C using an Amicon® Ultra Centrifugal Device (Millipore Inc., molecular weight cut-off (MWCO) of 12 kDa).

2.9. Determination of particle size, PDI and zeta potential

Particle size analyzer, Zetasizer (Malvern Zeta Sizer, Malvern Instruments, Malvern, UK) was utilized to evaluate the particle size, PDI and zeta potential of all the SLN formulations [21]. The measurements were carried out at a scattering angle of 90° at 25 °C. Prior to analysis, the SLNs was diluted in water accordingly to achieve a suitable count rate. In the determination of the particle size, Z-average (d.nm) with intensity (%) was used.

2.10. Encapsulation efficiency and drug loading determination

Indirect method was applied to determine the encapsulation efficiency of the compounds, by quantifying the free compounds [21]. Due to the low solubility of the compounds in water, the insoluble free compounds were initially collected by centrifugation at 7500 rpm for 30 min. The precipitate materials were dissolved in methanol and analyzed using HPLC. The free-dissolved compounds were quantified by determining the compounds from the filtrate from the purification step to concentrate the SLNs using HPLC. The encapsulation efficiency and drug loading of both compounds were calculated using the following equation:

$$\text{Drug loading (\%)} = \frac{\text{Amount of encapsulated compound}}{\text{Total weight of final formulation}} \times 100\%$$

2.11. FTIR study

To evaluate the possible intervention between the compounds in extract and excipients used to prepare SLNs, FTIR spectrophotometer (Shimadzu® FTIR-8400) was used [21]. In this study, extract, lipid, the physical mixture, and SLNs were scanned between 4000 and 600 cm^{-1} wavenumbers. Specifically, the measurements were carried out with a mirror speed of 0.05 cm/s and a resolution of 8 cm^{-1} . The FTIR spectrum was obtained from an average of 64 scans.

2.12. DSC evaluation

The thermal properties of the compounds in extract, as well as in SLNs formulation were evaluated using differential scanning calorimetry (DSC) (DSC 2920 (TA Instruments)) [21]. Extract, lipid, the physical mixture, and SLNs were weighed of around 5 mg and were closed in aluminum pan. The evaluation was performed from 25 to 300 $^{\circ}\text{C}$ with a flow rate of 10 $^{\circ}\text{C}/\text{min}$ under N_2 flow (40 mL/min).

2.13. XRD study

X-Ray diffractometer (Rigaku Corporation, England) was used to analyze the solid-state of the compounds in extract, as well as in SLNs formulation [37]. Extract, lipid, the physical mixture, and SLNs were scanned from 5 $^{\circ}$ to 50 $^{\circ}$ (2 θ) with a step scan speed of 5 $^{\circ}/\text{min}$. All samples were measured at a sampling width of 0.02 $^{\circ}$.

2.14. SEM evaluation

In this study, the morphologies of SLNs were detected using a scanning electron microscope (SEM) (JEM-1400Plus; JEOL, Tokyo, Japan) [44].

2.15. Solubility analysis

In order to investigate the solubility of both compounds in extract and SLN preparations, two different solvents, namely water and n-octanol were used [12]. Briefly, extract and SLNs were added in an excess amount to 5 mL of solvents. The mixture was stirred for 1 h at room temperature at 500 rpm. The supernatant was collected by centrifugation at 3000 rpm for 15 min and analyzed using HPLC.

2.16. In vitro drug release and mathematic models

The release of the compounds from the lipid matrix was carried out using the dialysis method was used [45–48]. Both HP β CD-modified and non-modified SLNs were used in this study. Additionally, the release of the compounds from the pure extract was also conducted. In this study, phosphate buffer saline (PBS) (pH 7.4) containing 1 % w/v of Tween 80 was used as a release medium to achieve sink condition during the release. Initially, the formulations were sealed inside the dialysis membrane (Spectra-Por®, 12,000–14,000 MWCO, Spectrum Medical Industries, CA, USA). The membrane was placed in 100 mL of release medium. The study was conducted at 37 $^{\circ}\text{C}$ at 100 rpm for 24 h. At each interval time, 1 mL of medium was withdrawn and replaced with similar volume of fresh media. The concentration of both compounds was analyzed using HPLC.

To further analyze the mathematic model kinetic, the release profiles were fitted to various models, including zero order, first order, Higuchi, Korsmeyer-Peppas and Hixson-Crowell. The calculation was performed using DDSolver (China Pharmaceutical University, Nanjing, China).

2.17. Stability evaluation in gastric environment

The stability of both HP β CD-modified and non-modified SLNs was

Table 3

Formulation chart of SLNs loaded dry floating in-situ gel system (%w/w).

Composition	FF1	FF2	FF3	FF4	FF5
SLNs	25	25	25	25	25
Gellan gum	5	5	5	5	5
Pluronic F127	2.5	5	7.5	10	15
Sodium citrate	1.5	1.5	1.5	1.5	1.5
Calcium carbonate	2.5	2.5	2.5	2.5	2.5
Microcrystalline cellulose	61	56	51	46	41

assessed in FaSSGF media [12]. The formulations were mixed with 10 mL of FaSSGF and incubated at 37 $^{\circ}\text{C}$. At 2 h, 4 h, 6 h and 8 h, the particle size, PDI and zeta potential of all formulations were determined.

2.18. Hemolytic evaluation

To assess the possibility of the formulation to cause any toxicity, in vitro hemolytic assay was conducted [49,50]. A fresh red blood cells (RBC) from Wistar rats was used in this study after three times washing steps. The RBS was prepared in a concentration of 10 % v/v in PBS. Briefly, 900 μL of RBC was mixed with 100 μL of samples. The mixture was incubated for 1 h. at 37 $^{\circ}\text{C}$ and spun for 10 min at 7000 rpm. The supernatant was collected, and the absorbance was detected using UV-Vis Spectrophotometer at 540 nm. The percentage of hemolysis was calculated using the following equation.

$$\text{Hemolysis (\%)} = \frac{\text{Abs samples} - \text{Abs negative control}}{\text{Abs positive control} - \text{Abs negative control}} \times 100\%$$

In this evaluation, PBS (7.4) and water were used as positive and negative control, respectively.

2.19. Formulation of SLNs loaded dry floating gel in-situ

Prior to the preparations, the concentrated SLNs were initially freeze dried with the addition of 2.5 % w/v trehalose as a cryoprotectant. Dry floating gel in situ was prepared using the composition depicted in Table 3. All formulations contained lyophilized SLNs, gellan gum, Pluronic F127, sodium citrate, calcium carbonate and microcrystalline cellulose. All the components were mixed using dry blender and further evaluated for their characterizations.

2.20. Angle of repose determination

The assessment of angle of repose of the dry formulation was carried out using funnel method [32]. The funnel was initially fixed on a stand. Briefly, the powder was placed in the powder funnel until all the powder passed the funnel. Afterwards, the diameter of the height of the dry formulation under the funnel were measured. The angle of repose was calculated using the following calculation:

$$\text{Angle of repose} = \tan^{-1} \frac{\text{Height}}{\text{Diameter}} \times 2$$

2.21. In vitro gelation study

The gelation properties of the formulations were carried out by dispersing the dry powder into distilled water in a ratio 1:5. Following this, the dispersion (5 mL) was carefully added into FaSSGF media (100 mL) inside the glass Beaker under the stirring at 50 rpm at 37 \pm 0.5 $^{\circ}\text{C}$. The time required by the liquid formulation to form a gel was observed and recorded as gelation time [51].

2.22. In vitro floating study

The formulation was evaluated for the floating study using USP Dissolution Apparatus. Firstly, the dispersion of the formulation (10 mL)

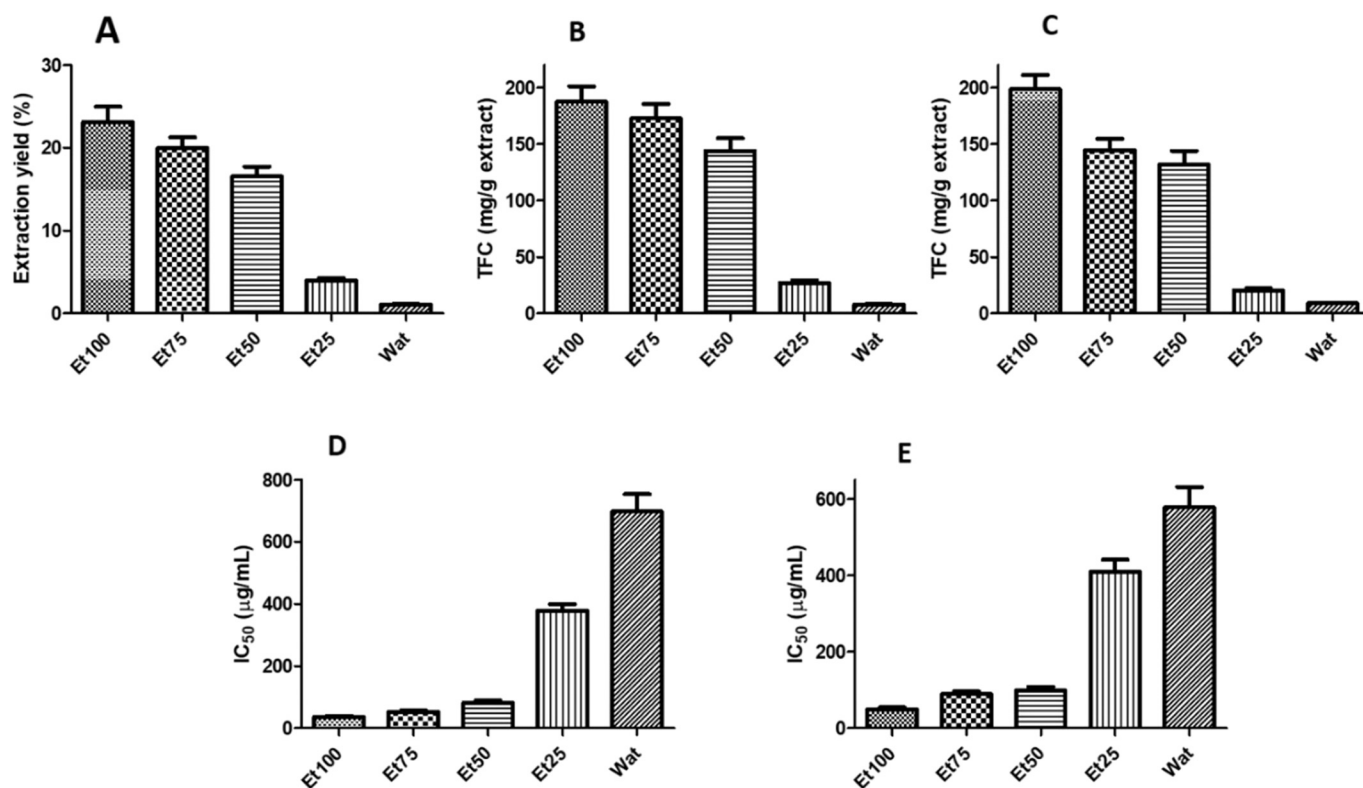


Fig. 1. Extraction yield (A), TFC (B), TPC (C), IC₅₀ values against DPPH (D) and IC₅₀ values against lipid peroxidation (E) of safflower extract obtained from different solvents (mean \pm SD, $n = 3$).

was put into opened Petri dish. Afterwards, the dish was put into FaSSGF media (100 mL) inside the dissolution vessel at 37 ± 0.5 °C. The floating lag time was recorded by observing the time required by the gel formed to float on the surface. Furthermore, the floating duration time was also recorded by observing the time required by the gel to stop floating [51].

2.23. Measurement of viscosity and gel strength

Prior to the evaluations, the formulation was dispersed in 100 mL, and 10 mL of the formulation was placed in the 100 mL of FaSSGF media, forming gel structure. The viscosity of the formulation was assessed using a rheometer (AR-2000ex rheometer, TA Instruments, UK). The determination was conducted using the oscillatory method with 0.5 mm trim gap and parallel plate of 50 mm. Initially, the formulation was placed into the bottom part of the instrument and the sample shearing was decreased using the trim gap. The determination was carried out at 25 °C at 1 Hz frequency. Furthermore, to assess the gel strength, the frequency sweep was carried out using 1 % strain at 37 °C. The analysis was performed between 0.05 and 10 Hz of frequency. The gel strength was indicated by the value of the ratio of the modulus of storage (G') and the modulus of loss (G'') (G'/G'' value) [52,53].

2.24. Preparation of dissolution media

Two different types of dissolution media were used, namely FaSSGF (Fasted-State Simulated Gastric Fluid) and FeSSGF (Fed-State Simulated Gastric Fluid). The preparation of FaSSGF was carried out by solubilizing 1.999 g of NaCl in 1000 mL of purified water. The pH of the solution was adjusted to 1.5 using HCl 1 M [12]. Meanwhile, the preparation of FeSSGF was carried out by mixing skimmed milk and acetate buffer pH 5.0 at a ratio of 1:1. To mimic the pH of fed state in the gastric, the pH of the mixture was adjusted to pH 5 using 1 M HCl [54].

2.25. In vitro drug dissolution study

The dissolution study of both compounds in safflower extract from the formulation was carried out using USP Dissolution Apparatus II (paddle). Initially, the dissolution vessel was filled with 900 mL of FaSSGF. Then, following the dispersion of the dry formulation in water, the formulation (10 mL) was put into dissolution media. At pre-determined interval times, 5 mL of the media was taken, replaced with the fresh media and the amount of both compounds was analyzed using HPLC. The study was carried out at 50 rpm at 37 ± 0.5 °C. Additionally, the dissolution of both compounds in three different conditions was performed, as previously reported in our study, namely the FeSSGF and FaSSGF after being released in 2 h in FaSSGF [37]. The release profiles of both compounds from crude extract-loaded dry floating gel in situ and non-decorated SLNs were also investigated.

2.26. Statistical analysis

The statistical analysis of all results was carried out using GraphPad Prism® version 6 (GraphPad Software, San Diego, California, USA). Statistically different was denoted when $p < 0.05$. Where appropriate, an independent and an unpaired t -test was used to compare two groups. Specifically, The Kruskal-Wallis test with post-hoc Dunn's test was applied to compare data from multiple groups.

3. Results and discussion

3.1. Extraction yield, TFC and TPC of safflower extract

Safflower has been found to show strong antioxidant properties against free radicals. This is related to the rich flavonoid and phenolic compounds in safflower [17,19,20]. It has been previously reported that both compounds and their glycoside forms can protect the damage caused by an oxidative reaction from free radicals [16–20]. In our study,

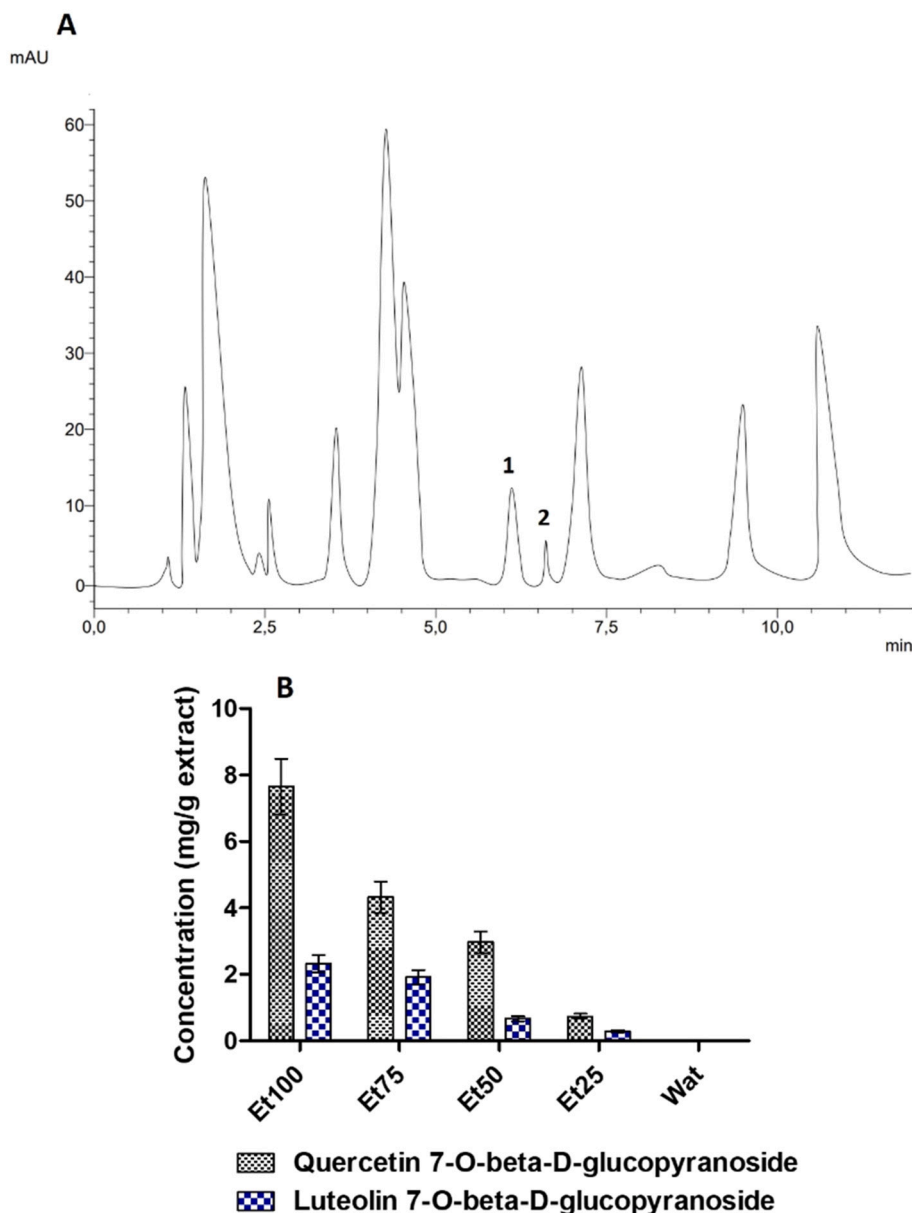


Fig. 2. HPLC chromatogram of quercetin 7-O-beta-D-glucopyranoside (1) and luteolin 7-O-beta-D-glucopyranoside (2) in safflower extract (A). Concentration of both compounds safflower extract obtained from different solvents (B) (mean \pm SD, $n = 3$).

initially, we extracted safflower using different solvents, mainly containing ethanol and water. The yield of the extraction, TFC, TPC, and antioxidant properties of all extract are depicted in Fig. 1. It was found that the high concentration of ethanol was able to increase the extraction yield, TFC and TPC. The highest values were achieved by the use of Et100 as extraction solvent. The extraction yield, TFC and TPC of Et100 were found to be 23.12 ± 1.87 % w/w, 187.37 ± 13.87 mg/g extract (equal to quercetin) and 198.43 ± 12.87 mg/g extract (equal to gallic acid), respectively. The difference in solvent type could significantly affect the extract yield, TFC and TPC ($p < 0.05$). Accordingly, the bioactive compounds, including flavonoid and phenolic contained in safflower possessed low solubility in water which could further limit its application.

3.2. Antioxidant activity using DPPH

Furthermore, as the main purpose of this study was related to antioxidant properties, the antioxidant activities of all extract were assessed.

Antioxidant could have various benefits in medical applications, particularly the condition triggered by oxidative stress from free radical. In our study, the antioxidant activities of safflower extract were in good agreement with the results from TFC and TPC determination. Using DPPH as free radical, in comparison with other extracts, Et100 possessing the highest TFC and TPC showed the lowest IC₅₀ value, implying its strongest antioxidant behavior. This could be explicated that both flavonoid and phenolic compounds in safflower could act as antioxidant agents. The IC₅₀ values of Et100, Et75, Et50, Et25 and Wat are depicted in Fig. 1D, showing the values of 36.87 ± 2.81 μ g/mL, 52.91 ± 4.69 μ g/mL, 81.98 ± 7.53 μ g/mL, 378.28 ± 21.17 μ g/mL and 698.43 ± 54.93 μ g/mL, respectively. Analyzed statistically, there was a statistical difference in IC₅₀ values of all extracts ($p < 0.05$).

3.3. Antioxidant activity using lipid peroxidation

The antioxidant properties of all extracts were also investigated using the lipid peroxidation method. As lipids are the major component

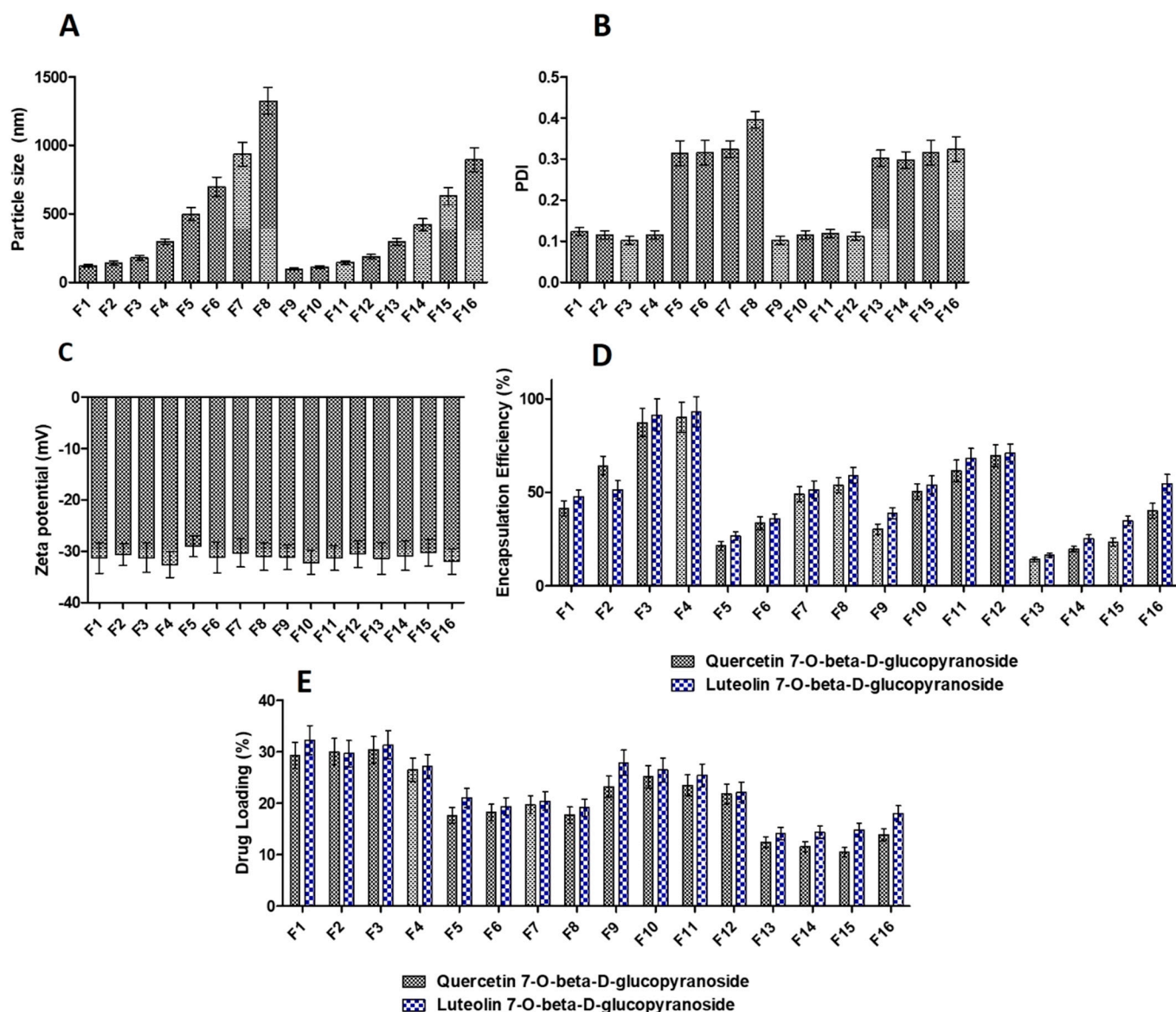


Fig. 3. Particle size (A), PDI (B), zeta potential (C), encapsulation efficiency (D) and drug loading (E) results of SLNs prepared from safflower extract (mean \pm SD, $n = 3$).

of the cell membrane, this method represents the ability of the compounds to protect the damage of the cell membrane caused produced by peroxy radicals [43]. In this evaluation, it was found that the IC₅₀ of Et100, Et75, Et50, Et25 and Wat against lipid peroxidation were $48.75 \pm 3.42 \mu\text{g/mL}$, $89.04 \pm 6.56 \mu\text{g/mL}$, $98.97 \pm 8.91 \mu\text{g/mL}$, $409.51 \pm 31.67 \mu\text{g/mL}$ and $577.43 \pm 43.87 \mu\text{g/mL}$, respectively (Fig. 1E). Similar to the DPPH test, the difference in solvent type significantly influenced the IC₅₀ values in lipid peroxidation method ($p < 0.05$).

3.4. HPLC analysis of active compounds

The investigation was intended to encapsulate the safflower extract into SLNs delivery system for further incorporation into floating in situ system. It was important to analyze the interest compound in safflower extract. In this study, quercetin 7-O-beta-D-glucopyranoside and luteolin 7-O-beta-D-glucopyranoside were used as the interest compounds, analyzed using HPLC. The chromatogram of both compounds and the concentration in all extracts are depicted in Fig. 2A. The concentrations of quercetin 7-O-beta-D-glucopyranoside in safflower extract were $7.65 \pm 0.63 \text{ mg/g}$ for Et100, $4.32 \pm 0.32 \text{ mg/g}$ for Et75, $2.97 \pm 0.19 \text{ mg/g}$

for Et50, $0.74 \pm 0.05 \text{ mg/g}$ for Et25 and $0.02 \pm 0.001 \text{ mg/g}$ for Wat. Moreover, the concentrations of luteolin 7-O-beta-D-glucopyranoside of Et100, Et75, Et50, Et25 and Wat were $2.32 \pm 0.21 \text{ mg/g}$, $1.92 \pm 0.15 \text{ mg/g}$, $0.67 \pm 0.05 \text{ mg/g}$, $0.29 \pm 0.03 \text{ mg/g}$ and $0.01 \pm 0.001 \text{ mg/g}$, respectively. From these results, it was shown that the concentrations of both compounds were very low in Wat (Fig. 2B), due to the non-polar properties. Importantly, Et100 produced the highest concentrations of both interest compounds. Taking into consideration of the results from extraction yield, TFC, TPC and antioxidant activity evaluations, this extract was used for further experiments.

3.5. Solid lipid nanoparticles preparation and characterizations

In an attempt to enhance the solubility and bioavailability of the compounds in safflower extract, it was incorporated into SLNs formulation decorated with HP β CD. In this study, Geleol® was selected as lipid matrix. In our preliminary study (data not shown), we previously screened different types of lipids, namely, Compritol® 888 ATO, Precirol® ATO 5 and stearic acid. According to the particle size and encapsulation efficiency values, other lipids were not able to produce

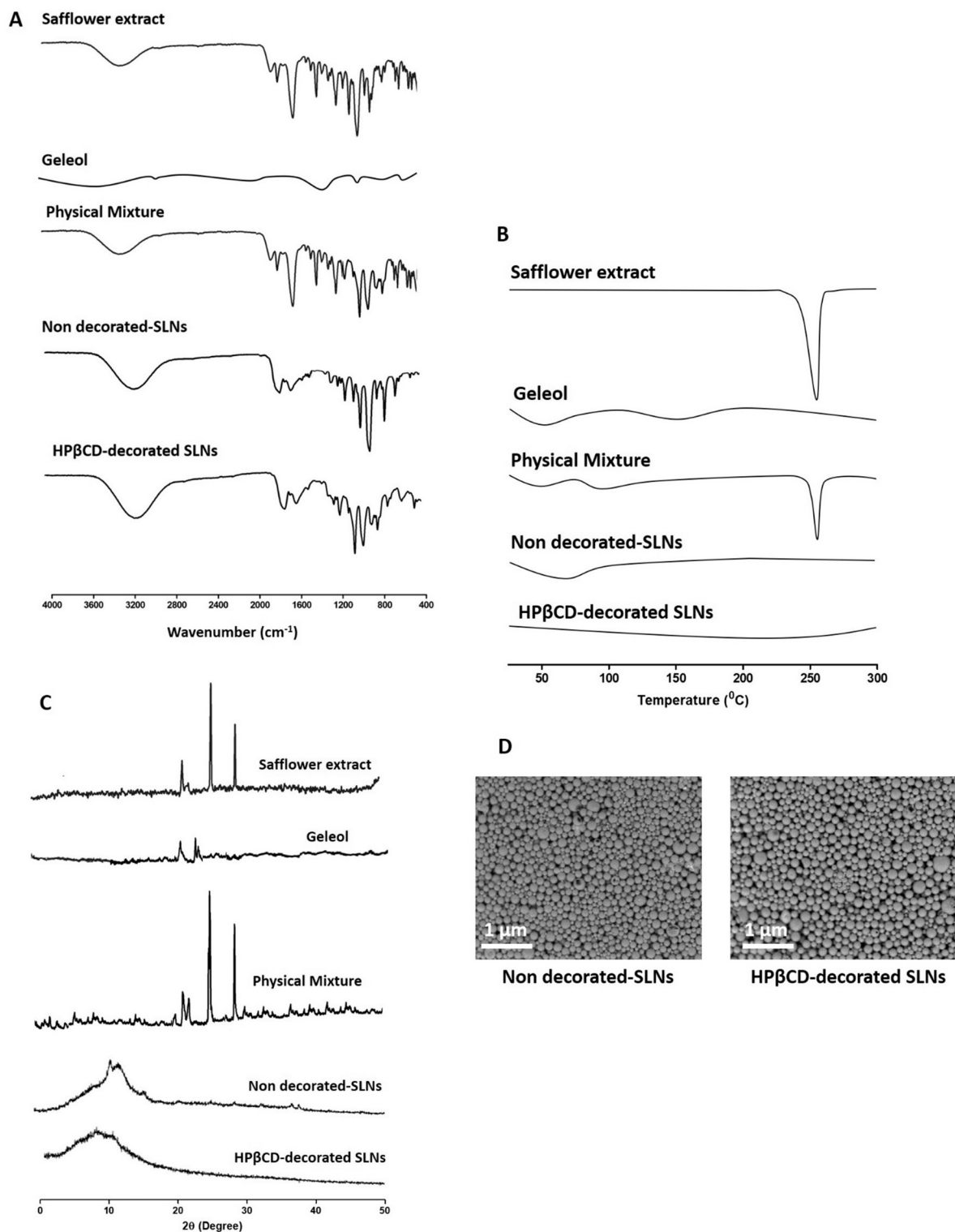


Fig. 4. The results of FTIR (A), DSC (B), XRD (C) and SEM (D) evaluations.

desire particle sizes and encapsulation efficiencies. With respect to the size, compared to other lipids, Geleol®, produce the smallest particle sizes. This might be due to the lowest melting point of Geleol®, causing the low viscosity in the solvent and when mixed with stabilizer solution. In our preliminary study, we found that the viscosity of the dispersion of Compritol® 888 ATO, Precirol® ATO 5 and stearic acid were 198.54 mPa.s, 243.18 mPa.s and 319 mPa.s, respectively. The low viscosity could improve the sonication effectiveness, resulting in smaller particle

sizes compared to other lipids [43]. Regarding the encapsulation efficiency, the higher encapsulation of SLNs prepared from Geleol® might be caused by the ability of hydroxyl group of glycerols as hydrogen bond donor functional groups contained in Geleol® to form hydrogen bonds with hydrogen bond receiver functional groups of Quercetin 7-O-beta-D-glucopyranoside and Luteolin 7-O-beta-D-glucopyranoside. This formation could generate a molecular complex, resulting in improved solubilization of both compounds in Geleol® [55]. Therefore, this

increased the encapsulation efficiency of both compounds in lipid matrix.

In this study, several parameters were evaluated to achieve SLNs with desired characteristics. The particle size, PDI, and zeta potential values of all formulations are shown in Fig. 3A–C. Moreover, the encapsulation efficiencies of quercetin 7-O-beta-D-glucopyranoside and Luteolin 7-O-beta-D-glucopyranoside are depicted in Fig. 3D. Initially, we evaluated the effect of lipid matrix concentration. It was found that the increment of lipid concentration could increase the particle size and encapsulation efficiency. However, the increase of lipid from 200 mg (F3) to 250 mg (F4) did not improve the encapsulation efficiency ($p > 0.05$) while increasing the particle size significantly ($p < 0.05$). The effect of different types of stabilizers, namely Tween80 and PVA, was also observed. The results showed that Tween80 could produce smaller particle size and higher encapsulation efficiency compared to PVA. It might be due to the difference in HLB values. It has been previously described that the HLB values of between 12 and 16 could form a stable oil-in-water (O/W) emulsion, leading to smaller droplet of nanoparticles formed [56]. As the HLB of Tween80 and PVA were >24 and 15, respectively, SLNs prepared Tween80 were smaller in size. The effect of sonication time was also studied, showing that the increase of sonication time could reduce the particle size of nanoparticles. However, this could reduce the encapsulation efficiency and drug loading of both compounds in SLNs matrix. This might be caused by the increase of the small droplet number and the separation of the generation of the core-shell of the nanoparticles. This could result in escape of the encapsulated compounds during the emulsification process, decreasing the encapsulation efficiency and drug loading of both compounds in lipid matrix [43]. Additionally, it was found that all SLNs produced zeta potential of around -30 mV, indicating the high stability of SLNs. The negative charge of SLNs might be due to the anionic nature of the lipid [21]. Following the optimization process, F3 prepared from 200 mg of Geleol® and 100 mg of extract, stabilized with 1 % of Tween80 and sonicated for 10 min was selected as the optimum formulations. The SLN possessed particle size, PDI, and zeta potential of 178.97 ± 16.57 nm, 0.102 ± 0.01 , -31.24 ± 2.87 mV, respectively. The encapsulation efficiency values of quercetin 7-O-beta-D-glucopyranoside and luteolin 7-O-beta-D-glucopyranoside were found to be 87.31 ± 7.65 % and 91.36 ± 8.61 %. Moreover, the drug loading values of quercetin 7-O-beta-D-glucopyranoside and luteolin 7-O-beta-D-glucopyranoside were found to be 30.65 ± 2.19 % and 31.34 ± 2.86 %. This formulation was further decorated using HP β CD. As previously explained, was used to decorate the SLNs to improve the stability especially in the gastrointestinal tract [26,29]. Using similar preparation process, the decorated SLNs possessed particle size of 187.36 ± 12.02 nm, PDI of 0.114 ± 0.01 and zeta potential of -30.25 ± 2.14 mV. The encapsulation efficiencies were 86.98 ± 7.12 % for Quercetin 7-O-beta-D-glucopyranoside and 90.78 ± 7.83 % for Luteolin 7-O-beta-D-glucopyranoside. Furthermore, the drug loading capacities were 29.54 ± 2.16 % for Quercetin 7-O-beta-D-glucopyranoside and 29.88 ± 2.54 % for Luteolin 7-O-beta-D-glucopyranoside. It was found that following the incorporation of HP β CD, importantly, the properties of SLNs did not change significantly ($p > 0.05$).

3.6. FTIR study

FTIR study was conducted to investigate the possible interaction between interest compounds and all the excipients used in the formulation. As shown in Fig. 4A, safflower extract showed at 3239 cm^{-1} due to the vibration of -OH functional groups of the phenolic parts of both compounds. Additionally, another peak was detected at 1684 cm^{-1} which might be due to the presence of C=O stretching of the ketone carbonyl. Distinct peak was observed at 1614 cm^{-1} due to -C-O stretching of quercetin 7-O-beta-D-glucopyranoside and central heterocyclic ring of luteolin 7-O-beta-D-glucopyranoside. Other peaks were found at 1519 cm^{-1} , 1363 cm^{-1} and 1237 cm^{-1} due to C-C=C

Table 4

The solubilities of interest compounds in water and n-octanol from extract, SLNs and HP β CD-SLNs (mean \pm SD, $n = 3$).

Compound	Samples	Aqueous solubility ($\mu\text{g}/\text{mL}$)	n-Octanol solubility ($\mu\text{g}/\text{mL}$)
Quercetin 7-O-beta-D-glucopyranoside	Extract	18.32 ± 1.32	408.45 ± 29.34
	SLNs	278.43 ± 20.31	411.23 ± 31.72
	HP β CD-SLNs	301.21 ± 26.32	415.87 ± 33.67
Luteolin 7-O-beta-D-glucopyranoside	Extract	16.54 ± 1.36	434.73 ± 39.42
	SLNs	201.23 ± 17.44	454.31 ± 40.38
	HP β CD-SLNs	243.12 ± 21.27	461.21 ± 38.17

asymmetric stretch, C-OH stretch and C-O-C bond, respectively. All the peaks were also detected in both physical mixture and SLN formulations. Interestingly, the peak at 3239 cm^{-1} was found to be broader, which might be due to the formation of hydrogen bonding between lipid matrix and interest compounds. It should be noted that the spectrums observed in the extract between 1100 and 1200 cm^{-1} were not identified in the SLNs following the purification step. This indicated that the method could remove unencapsulated compounds, while maintaining the presence of the interest compounds inside the lipid matrix.

3.7. DSC analysis

Fig. 4B shows the DSC thermograms of safflower extract, the physical mixture, and both SLN formulations. As shown in the thermogram, safflower extract showed a sharp peak at 252 $^{\circ}\text{C}$ due to the melting point of quercetin 7-O-beta-D-glucopyranoside and luteolin 7-O-beta-D-glucopyranoside which also showed the crystalline form of the compounds. In the case of Geleol, broad peak was observed at 61 $^{\circ}\text{C}$, representing the melting point of the lipid. Following the observation in the physical mixture, the peaks were still identified, showing that all compounds did not change when mixed physically. In the SLN formulations, the sharp peak was not observed, showing the formation of the crystalline compounds to amorph. Additionally, this could also show that all compounds were successfully entrapped inside the lipid matrix [21]. The transformation of the crystalline form to amorphous could be beneficial in the enhancement of the solubility of the hydrophobic compounds.

3.8. XRD analysis

In good agreement with DSC thermograms, XRD evaluations showed distinguishable peaks around 20 – 35 $^{\circ}2\theta$ regions (Fig. 4C), showing the crystallinity of the compounds. Furthermore, these peaks were not found in SLN formulations, indicating the amorphous state of the system developed in this study. In the XRD pattern of Geleol, the small peaks were observed between 20 and 25° , demonstrating the low crystallinity of the lipid. The XRD analysis data was in a good agreement with the DSC analysis, showing that the presence of the peaks in the physical mixture and the absence of the peaks in the SLNs, showing the formation of amorphous SLNs.

3.9. Solubility analysis

The formulation of hydrophobic compounds into SLNs has been widely reported to improve the solubility of the compounds. Table 4 showed the comparison of the inherent solubility values in water and n-octanol of quercetin 7-O-beta-D-glucopyranoside and luteolin 7-O-beta-D-glucopyranoside in safflower extract and SLN formulations. As depicted, due to their hydrophobicity, the water solubility values of both compounds were 18.23 ± 1.32 $\mu\text{g}/\text{mL}$ and 16.54 ± 1.36 $\mu\text{g}/\text{mL}$ for quercetin 7-O-beta-D-glucopyranoside and luteolin 7-O-beta-D-glucopyranoside, respectively. On the other hand, significant higher ($p <$

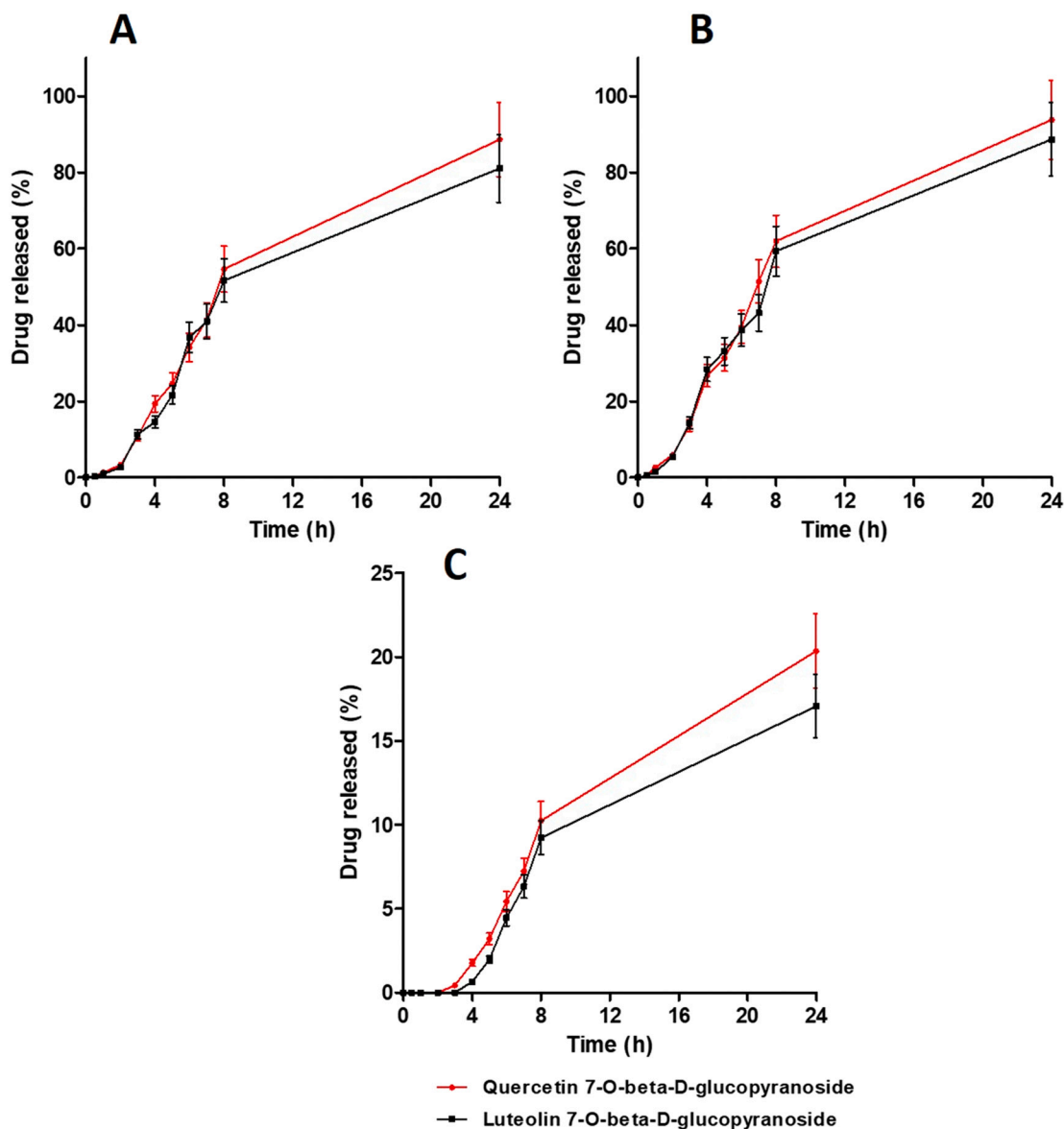


Fig. 5. In vitro release profiles of quercetin 7-O-beta-D-glucopyranoside and luteolin 7-O-beta-D-glucopyranoside from non-decorated SLNs (A), HPβCD-decorated SLNs (B) and extracts (C) (mean \pm SD, $n = 3$).

0.05) solubility values were found in n-octanol, namely 408.45 ± 29.34 $\mu\text{g/mL}$ and 434.31 ± 39.31 $\mu\text{g/mL}$. Following the incorporation into SLNs, the water solubility increased significantly ($p < 0.05$) up to approximately 15-fold for both compounds. Furthermore, the solubilities of these compounds were also enhanced in n-octanol, despite non-significant ($p > 0.05$) increment. Furthermore, following the decoration using HPβCD, due to the solubilization enhancement ability of HPβCD [57], the solubility of both compounds in decorated SLNs was higher compared to non-decorated SLNs. However, there was no significant different ($p > 0.05$) in the solubility values.

This evaluation confirmed that the formulation of SLNs was able to enhance the solubility of hydrophobic compounds in safflower extract. Numerous studies have shown that the reduction of the size in nanoparticles could potentially enhance the solubility of hydrophobic drugs in many cases [58–62].

3.10. In vitro drug release and mathematic models

In this study, dynamic dialysis using dialysis membrane was applied to evaluate the release of both compounds from SLNs. Fig. 5 depicts the

cumulative release of quercetin 7-O-beta-D-glucopyranoside and luteolin 7-O-beta-D-glucopyranoside from non-decorated SLNs and HPβCD-decorated SLNs. Overall, it was found that the incorporation of safflower extract into SLNs could improve and sustain the release patterns of both compounds. For Quercetin 7-O-beta-D-glucopyranoside, only 0.43 ± 0.03 % of compound were released from extract after 3 h. No compound was detected in the first 2 h. After 24 h, the release percentage was found to be 20.35 ± 1.87 %. In the SLN formulations, after 3 h, 10.69 ± 1.19 % and 12.98 ± 1.21 % of compound were released from non-decorated SLNs and HPβCD-decorated SLNs, respectively. The releases were sustained over 24 h, reaching the final release percentages of 88.63 ± 7.87 % and 93.76 ± 8.18 %, respectively. In terms of the release profile of luteolin 7-O-beta-D-glucopyranoside, the release was found after 4 h from the extract, which was only 0.65 ± 0.05 %. In case of SLN formulations, the release percentages were 11.36 ± 1.27 % for non-decorated SLNs and 14.32 ± 1.29 % for HPβCD-decorated SLNs. Similar to another compound, sustained release behavior was also observed after 24 h, showing that 81.06 ± 7.65 % and 88.69 ± 8.01 % of the compound were released from both SLNs, respectively. Specifically, it was observed that during the first 3 h, there was a fast release pattern

Table 5

The particle size (nm) of non-decorated SLNs and HP β CD-decorated SLNs following several incubation times in FaSGGF (mean \pm SD, $n = 3$).

Samples	0 h	2 h	4 h	6 h	8 h
SLNs	178.97 \pm 16.57	193.83 \pm 12.12	234.56 \pm 20.18	382.28 \pm 21.82	476.12 \pm 38.89
HP β CD-SLNs	187.36 \pm 12.02	189.32 \pm 13.71	190.31 \pm 12.73	191.27 \pm 17.29	204.87 \pm 15.34

of both compounds from SLNs. This might be caused by the low percentage of compounds in the outer layer of lipid matrix, leading to the quick diffusion of both compounds into the release medium [63]. Following this, the slow-release pattern was observed. In an attempt to understand the release kinetic and mechanism of both compounds from SLNs matrix, the release profiles were fitted into release kinetic models. It was found that the release kinetic of both compounds followed Higuchi model with R values of >0.98 . Therefore, it could be explained that both compounds released from lipids due to the diffusion and the erosion process [21,49].

3.11. Stability evaluation in gastric environment

In order to investigate the stability of SLNs in the gastrointestinal tract, the characteristics of non-decorated SLNs were compared to HP β CD-decorated SLNs. The particle sizes, PDIs, zeta potentials of both formulations during the incubation in FaSGGF media are depicted in Table 5. It was shown that without the addition of HP β CD, there were significant improvements ($p < 0.05$) of the particle size during 8 h. On the other hand, following the decoration using HP β CD, the particle size did not change significantly ($p > 0.05$), indicating the improvement of the stability of SLNs following the decoration using HP β CD.

3.12. Hemolytic evaluation

Initial potential toxicity of nanoformulations could be assessed using in vitro hemolytic assay. This study was performed to investigate the ability of SLNs to lyse erythrocytes, indicating the toxicity. The results of this evaluation are depicted in Fig. 6. As shown, the hemolysis percentage values of both SLNs were below 5%. Accordingly, it can be

hypothesized that the SLNs developed in this study are considerably safe at the evaluated concentrations [47,48].

3.13. Formulation of SLNs loaded dry floating gel in-situ

In this study, we incorporated HP β CD-decorated SLNs into dry floating in situ gel using gellan gum. The dry formulation should be initially dispersed in water before the oral administration. The principle of in situ gelation formation is due to the reaction of gellan gum and divalent ions. Categorized as anionic polysaccharide, gellan gum solution forms gel in the existence of Ca $^{2+}$ [32]. In this formulation, following contact with the acidic condition in the gastric juice, calcium carbonate would be solubilized and release Ca $^{2+}$ which are further complexed by sodium citrate [37]. Additionally, the release of free Ca $^{2+}$ from the complex has been found to be slow, resulting in gelation of gellan gum. Additionally, following the release of Ca $^{2+}$ from calcium carbonate, carbon dioxide (CO $_2$) would be released and entrapped inside the gel network, decreasing the density of the system and causing the floating system in the gastric environment [64]. Additionally, Pluronic F127 was also used as thermogelling system which would also control the release of the compounds [65,66]. As a diluent of the dry formulation, microcrystalline cellulose was used, due to its ability to enhance the flow property of the system.

3.14. Angle of repose determination

As the main form of the system developed in this study was dry powder, it was crucial to evaluate its flowability. Here, repose angle was assessed to represent the flowability of the powder. As shown in Fig. 7A, all repose angles were above 25°, indicating the excellent flowability of dry powder formulation. Specifically, the angle of repose values was 35.76 \pm 2.98, 35.09 \pm 3.02, 33.82 \pm 3.21, 33.12 \pm 2.78 and 32.19 \pm 3.29 for FF1, FF2, FF3, FF4 and FF5, respectively. It was important to note that there was no significant difference ($p > 0.05$) in the values of the repose angles of all formulations.

3.15. Viscosity and gel strength determination

Furthermore, the viscosity of the pre-gelation dispersion was determined. The result is shown in Fig. 7B. The rheogram showed that all the

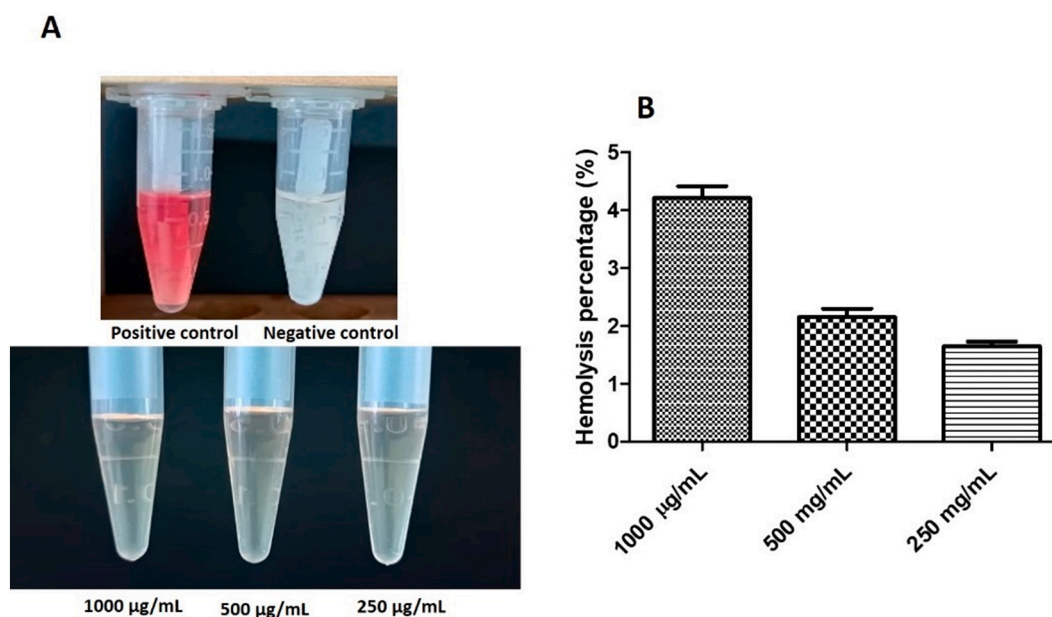


Fig. 6. Representative images of in vitro hemolysis evaluation (A) and hemolysis percentages of decorated SLNs in three different concentrations (B) (mean \pm SD, $n = 3$).

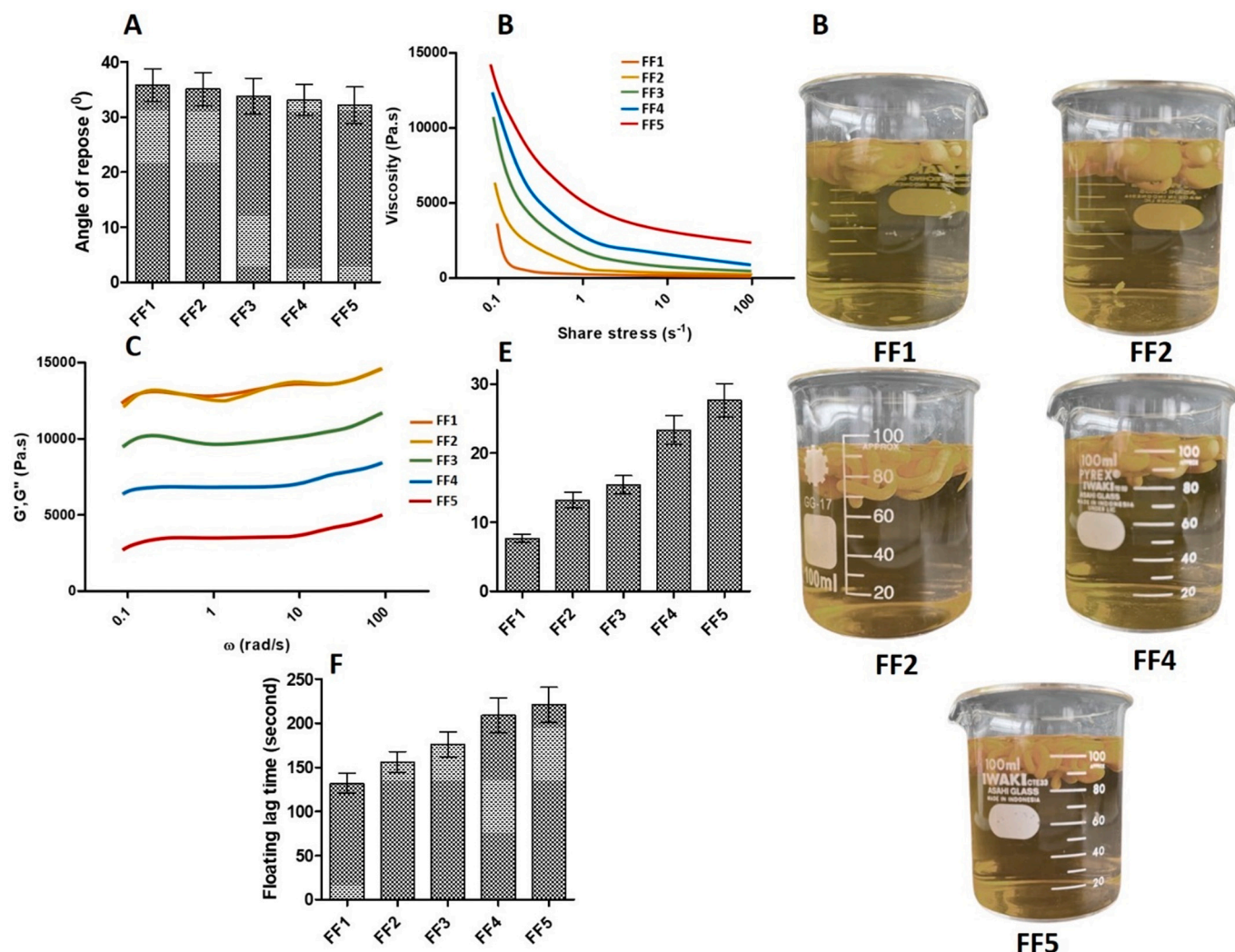


Fig. 7. Angle of repose (A), viscosity (B), gel strength (C), gelation time (D) and floating lag time (E) of SLNs loaded floating gel in situ (mean \pm SD, $n = 3$). Representative images of floating gel in situ (F).

formulations exhibited non-Newtonian behavior. Analyzed statistically, there was a significant difference ($p < 0.05$) in the viscosity value in all formulations. The difference in viscosity was caused by the use of Pluronic F127 as thermogelling agent. Several studies have explored the use of Pluronic F127 as gelling agent, causing the increase in viscosity with the increase of the concentrations [65,66].

The strength values of the gel formulation are shown in Fig. 7C. The value of $G'G''$ represented the strength of the gels. It was found that the increase of Pluronic F127 concentration from 2.5 % to 10 % could significantly improve ($p < 0.05$) the gel strength of the formulation. However, the increase from 10 % to 15 % ($p > 0.05$) did not show any significant improvement in the gel strength. This was in a good agreement with the viscosity determination, showing that the higher viscosity resulted in stronger gel strength. It was necessary to maintain rigid gel assembly in floating gel formulation. The drug loaded into the gel matrix would release to gastric environment depending on the strength of the complex 3D structure of the gel network [64]. Accordingly, the gel should be strong enough to maintain its integrity. The strength values of the gel were similar to the values reported previously, showing the ability of the formulation in maintaining the gel form in the gastric environment.

3.16. Gelation time

Gelation time is one of critical parameters in in situ gel formulation. In order to control the release of drugs, the formulation should be able to form gel before the release of the drugs from the gel matrix. Fig. 7D exhibits the time required by the formulation to form a gel structure, showing that all formulation were able to form a gel in FaSGGF media at body temperature < 30 s. As explained in previous section, gellan gum could form gel following the presence of Ca^{2+} release from calcium carbonate. Importantly, it was found that the concentration of Pluronic F127 could affect the gelation time of the formulation. The increase in Pluronic concentration ($p < 0.05$) could significantly decrease the gelation time of the formulation. Pluronic are water soluble nonionic triblock copolymers with polar and non-polar region, namely polyethylene oxide and poly propylene oxide, respectively. This polymer can undergo sol-to-gel conversion following the change of the temperature [49].

3.17. Floating lag time and duration of floating

Following the gel formation of the in situ formulation, to further sustain the release based on its gastroretentive characteristics, the formulation should be able to float in the gastric environment. Floating lag time represent this parameter and Fig. 7E depicts the floating lag

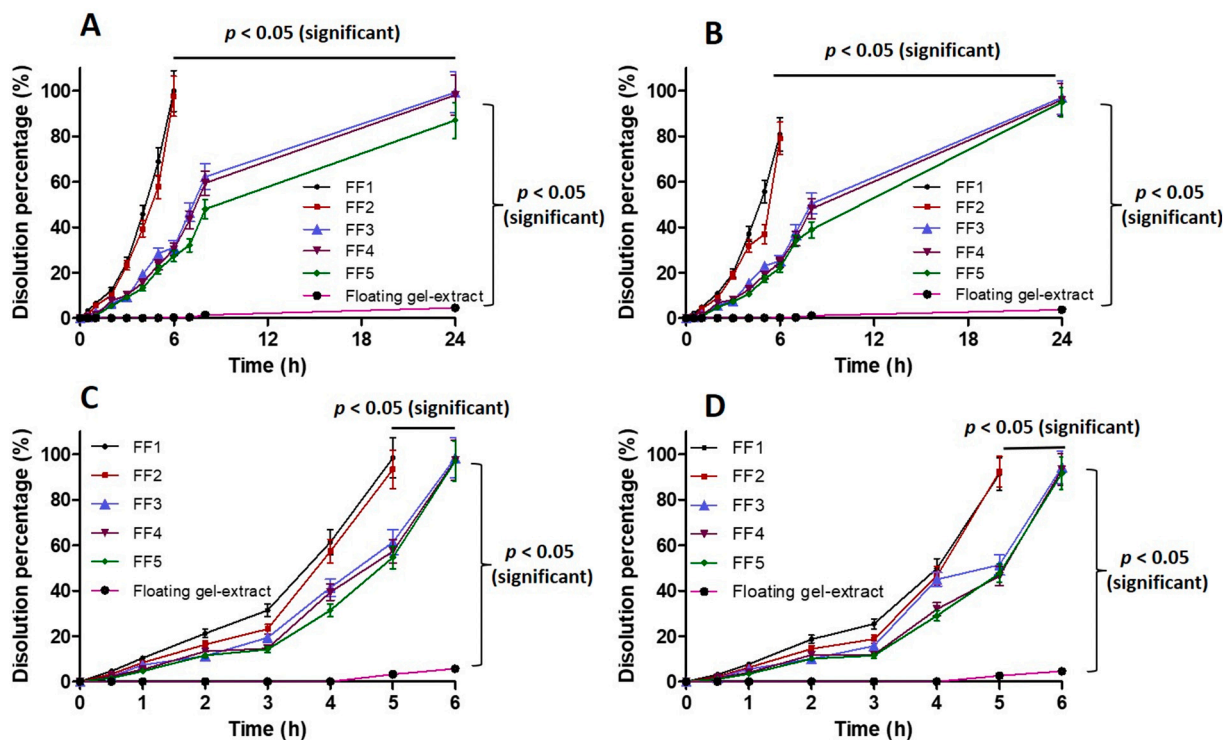


Fig. 8. In vitro dissolution profiles of quercetin 7-O-beta-D-glucopyranoside (A) and luteolin 7-O-beta-D-glucopyranoside (B) from SLNs loaded floating gel in situ system in FaSGGF, in vitro dissolution profiles of quercetin 7-O-beta-D-glucopyranoside (C) and luteolin 7-O-beta-D-glucopyranoside (D) from SLNs loaded floating gel in situ system in FeSGGF (mean \pm SD, $n = 3$).

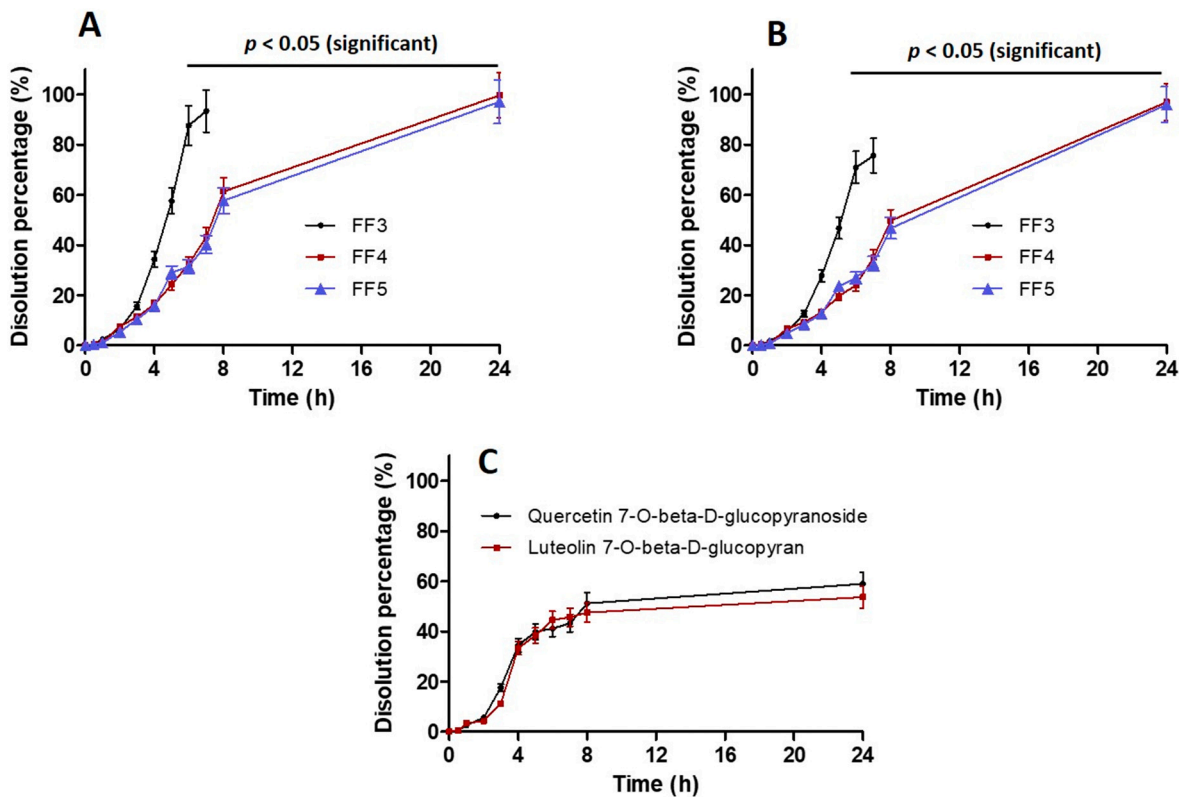


Fig. 9. In vitro dissolution profiles of quercetin 7-O-beta-D-glucopyranoside (A) and luteolin 7-O-beta-D-glucopyranoside (B) from SLNs loaded floating gel in situ system in FaSGGF after being released in FeSGGF for 2 h; in vitro dissolution profiles of quercetin 7-O-beta-D-glucopyranoside and luteolin 7-O-beta-D-glucopyranoside (C) from non-decorated SLNs loaded floating gel in situ system in FaSGGF after being released in FeSGGF for 2 h (mean \pm SD, $n = 3$).

times of the formulations. Following the concentration of Pluronic, the time required of the gelled formulation to float also increased. This might be associated with the increase of the viscosity of the formulation when the concentration of Pluronic increased. As a result, the penetration of the gastric fluid would decrease, retarding the reaction between the calcium carbonate with acid which affected the release of CO₂ [67]. A previous study has shown the same phenomenon showing that the floating lag time increased following the increase of the polymeric material in the system [68]. It should be noted that all formulations remained floating after 24 h (Fig. 7F).

3.18. *In vitro* drug dissolution study

The dissolution profile of quercetin 7-O-beta-D-glucopyranoside and luteolin 7-O-beta-D-glucopyranoside from SLNs incorporated into floating in situ formulation was investigated in three different conditions. To ensure that the formulation could control the dissolution of both compounds, the burst release should be avoided [69]. In this study, initially we evaluated the dissolution profile of Quercetin 7-O-beta-D-glucopyranoside and Luteolin 7-O-beta-D-glucopyranoside in FaSSGF. The dissolution profiles of both compounds in FaSSGF for 24 h are depicted in Fig. 8. The results showed that the incorporation of SLNs into floating gel in situ could potentially control the dissolution profile of active compounds from safflower extract. Without the SLNs formulation, the dissolution percentages were found to be significant lower ($p < 0.05$) in all cases. Specifically, the difference in Pluronic concentrations resulted in various control release patterns. As shown in Fig. 8A and B, below 7.5 % of Pluronic (FF1 and FF2), the sustained release patterns were only observed for 6 h. On the other hand, formulations containing 7.5 % (FF3), 10 % (FF4) and 15 % (FF5) of Pluronic were capable of controlling the release of the compounds over 24 h.

In FeSSGF, all formulations were not able to control the release of active compounds. As shown in Fig. 8C and D, all compounds were released <6 h. It was caused by the inability of gellan gum to form gel in the FeSSGF pH. Accordingly, this confirmed that the formulation should be taken in fast state. However, it was important to evaluate the effect of the release of active compounds from the developed formulations after food intake. In this investigation, only FF3, FF4 and FF5 were selected due to their ability to control the dissolution behavior for 24 h (Fig. 9A and B). After 2 h in FaSSGF, it was found that F3 with 7.5 % of Pluronic were not able to control the dissolution behavior of both compounds. On the other hand, FF4 and FF5 could potentially maintain and control the release of the active compounds encapsulated into SLNs. This could be related the difference in the gel strengths between the formulations. As the gel strength of FF3 was significantly lower ($p < 0.05$) than FF4 and FF5, the ability to maintain its rigid gel decreased when the formulation was moved into FaSSGF. Importantly, in this study, we also evaluated the dissolution profile of both compounds in the floating gel from the non-decorated SLNs. As shown in Fig. 9C the non-decorated SLNs were not able to control the release of both compounds. From 4 h onwards, there was no significant improvement of the dissolution percentages of both compounds. This could be the aggregation of the non-decorated SLNs following 4 h contact with the gastric environment (Table 5). Accordingly, this showed that it is crucial to decorate the SLNs using HPβCD to maintain the stability during the oral administration of this approach.

Overall, this study showed the possibility to improve the solubility of bioactive compounds in safflower using SLNs and further control the release using floating gel in situ system. As the data presented in our study is a proof of concept study in the biorelevant media, to further evaluate its efficacy, *in vivo* studies should now be conducted using appropriate animal model. The pharmacokinetic study is critical to investigate the effectiveness of this approach to improve the bioavailability of quercetin 7-O-beta-D-glucopyranoside and luteolin 7-O-beta-D-glucopyranoside in Safflower extract.

4. Conclusions

In this study, safflower extract with antioxidant activity was obtained using ethanol as extraction solvent. The extract showed antioxidant activity, expressed as IC₅₀ values of 36.87 ± 2.81 μg/mL against DPPH and 48.75 ± 4.52 μg/mL against lipid peroxidation. Specifically, the extract contained 7.65 ± 0.63 mg/g extract of quercetin 7-O-beta-D-glucopyranoside and 2.32 ± 0.21 mg/g extract of luteolin 7-O-beta-D-glucopyranoside. To improve the solubility, the extract was formulated into solid lipid nanoparticles (SLNs) decorated with hydroxypropyl beta-cyclodextrin (HPβCD) with particle size of 178.97 ± 16.57 nm, showing the improvement of 15-fold of solubility in water. The SLNs possessed gastric solubility with no particle size improvement after 8 h. The SLNs were further formulated into floating gel in situ delivery system using gellan gum as gelling agent. With desired gelation and floating properties, the formulation could control the release of quercetin 7-O-beta-D-glucopyranoside and luteolin 7-O-beta-D-glucopyranoside in biorelevant media. Furthermore, *in vivo* studies should be carried to explore the effectiveness of this approach in a suitable animal model.

CRedit authorship contribution statement

Conceptualization, A.D.P., A.R., F.N., and M.A.B.; methodology, A.D.P., A.S., and A.N.M.; software, A.D.P., A.S., A.N.M.; validation, A.D.P., A.R., and F.N.; formal analysis, A.S and A.N.M.; investigation, A.D.P., A.S., and A.N.M.; resources, A.D.P., A.R., and F.N.; data curation, A.D.P., A.S., A.N.M.; writing—original draft preparation, A.D.P.; writing—review and editing, A.R., F.N., and M.A.B.; visualization, A.D.P., A.S., and A.N.M.; supervision, A.D.P.; project administration, A.D.P.; funding acquisition, A.D.P., A.R., and F.N. All authors have read and agreed to the published version of the manuscript.

Funding

This study was supported by Ministry of Education, Culture, Research and Technology of Republic of Indonesia under Penelitian Dasar Kompetitif Nasional scheme, Number 090/E5/PG.02.00/PT/2022. The authors would like to thank Gattefosse Pvt. Ltd., France and Cyclolab Ltd., Budapest, Hungary for providing Geleol® and hydroxypropyl beta-cyclodextrin, respectively.

Declaration of competing interest

The authors declare that they have no known competing financial interests or personal relationships that could have appeared to influence the work reported in this paper.

References

- [1] T. Ebert, N. Tran, L. Schurgers, P. Stenvinkel, P.G. Shiels, Ageing – oxidative stress, PTMs and disease, *Mol. Asp. Med.* 86 (2022), 101099, <https://doi.org/10.1016/j.mam.2022.101099>.
- [2] D. Granato, Functional foods to counterbalance low-grade inflammation and oxidative stress in cardiovascular diseases: a multilayered strategy combining food and health sciences ☆, *Curr. Opin. Food Sci.* 47 (2022), 100894 <https://doi.org/10.1016/j.cofs.2022.100894>.
- [3] D. Li, G. Liang, R. Calderone, J.A. Bellanti, Vitiligo and Hashimoto's thyroiditis: autoimmune diseases linked by clinical presentation, biochemical commonality, and autoimmune/oxidative stress-mediated toxicity pathogenesis, *Med. Hypotheses* 128 (2019) 69–75, <https://doi.org/10.1016/j.mehy.2019.05.010>.
- [4] T. Gui, Y. Li, S. Zhang, I. Alecu, Q. Chen, Y. Zhao, T. Hornemann, G.A. Kullak-Ublick, Z. Gai, Oxidative stress increases 1-deoxysphingolipid levels in chronic kidney disease, *Free Radic. Biol. Med.* 164 (2021) 139–148, <https://doi.org/10.1016/j.freeradbiomed.2021.01.011>.
- [5] Y. Esmaili, Z. Yarjanli, F. Pakniya, E. Bidram, M.J. Los, M. Eshraghi, D.J. Klionsky, S. Ghavami, A. Zarrabi, Targeting autophagy, oxidative stress, and ER stress for neurodegenerative disease treatment, *J. Control. Release* 345 (2022) 147–175, <https://doi.org/10.1016/j.jconrel.2022.03.001>.
- [6] D. Rotariu, E.E. Babes, D.M. Tit, M. Moisi, C. Bustea, M. Stoicescu, A.F. Radu, C. M. Vesa, T. Behl, A.F. Bungau, S.G. Bungau, Oxidative stress – complex pathological issues concerning the hallmark of cardiovascular and metabolic

- disorders, *Biomed. Pharmacother.* 152 (2022), 113238, <https://doi.org/10.1016/j.biopha.2022.113238>.
- [7] M. Sanati, A.R. Afshari, P. Kesharwani, V.N. Sukhorukov, A. Sahebkar, Recent trends in the application of nanoparticles in cancer therapy: the involvement of oxidative stress, *J. Control. Release* 348 (2022) 287–304, <https://doi.org/10.1016/j.jconrel.2022.05.035>.
- [8] L. Sun, Y. Zhang, S. Wen, Q. Li, R. Chen, X. Lai, Z. Zhang, Z. Zhou, Y. Xie, X. Zheng, K. Zhang, D. Li, S. Sun, Extract of *Jasminum grandiflorum* L. alleviates CCl₄-induced liver injury by decreasing inflammation, oxidative stress and hepatic CYP2E1 expression in mice, *Biomed. Pharmacother.* 152 (2022), 113255, <https://doi.org/10.1016/j.biopha.2022.113255>.
- [9] D. Zhang, M. Dong, X. Song, X. Qiao, Y. Yang, S. Yu, W. Sun, L. Wang, L. Song, ROS function as an inducer of autophagy to promote granulocyte proliferation in Pacific oyster *Crassostrea gigas*, *Dev. Comp. Immunol.* 135 (2022), 104479, <https://doi.org/10.1016/j.dci.2022.104479>.
- [10] H. Udono, M. Nishida, Metformin-ROS-Nrf2 connection in the host defense mechanism against oxidative stress, apoptosis, cancers, and ageing, *Biochim. Biophys. Acta - Gen. Subj.* 1866 (2022), 130171, <https://doi.org/10.1016/j.bbagen.2022.130171>.
- [11] A. Siddeeq, N.M. AlKehayez, H.A. Abu-Hiamed, E.A. Al-Sanea, A.M. Al-Farga, Mode of action and determination of antioxidant activity in the dietary sources: an overview, *Saudi J. Biol. Sci.* 28 (2021) 1633–1644, <https://doi.org/10.1016/j.sjbs.2020.11.064>.
- [12] A.D. Permana, R.N. Utami, A.J. Courtenay, M.A. Manggau, R.F. Donnelly, L. Rahman, Phytosomal nanocarriers as platforms for improved delivery of natural antioxidant and photoprotective compounds in propolis: an approach for enhanced both dissolution behaviour in biorelevant media and skin retention profiles, *J. Photochem. Photobiol. B Biol.* (2020), <https://doi.org/10.1016/j.jphoto.2020.111846>.
- [13] A. Saraiva, A. Justino, R. Franco, H. Silva, F. Arruda, S. Klein, M. Celes, L. Goulart, F. Espindola, Polyphenols-rich fraction from *annona muricata* linn. leaves attenuates oxidative and inflammatory responses in neutrophils, macrophages, and experimental lung injury, *Pharmaceutics* 14 (2022) 1182, <https://doi.org/10.3390/pharmaceutics14061182>.
- [14] M. De Luca, D. Lucchesi, C.I.G. Tuberoso, X. Fernández-Busquets, A. Vassallo, G. Martelli, A.M. Fadda, L. Pucci, C. Caddeo, Liposomal formulations to improve antioxidant power of myrtle berry extract for potential skin application, *Pharmaceutics* 14 (2022), <https://doi.org/10.3390/pharmaceutics14050910>.
- [15] I. Faraone, L. Lela, M. Ponticelli, D. Gorgoglione, F. De Blasio, P. Valentão, P. B. Andrade, A. Vassallo, C. Caddeo, R. Falabella, A. Ostuni, L. Milella, New insight on the bioactivity of *Solanum aethiopicum* Linn. growing in Basilicata Region (Italy): phytochemical characterization, liposomal incorporation, and antioxidant effects, *Pharmaceutics* 14 (2022) 1168, <https://doi.org/10.3390/pharmaceutics14061168>.
- [16] I. Adamska, P. Biernacka, Bioactive substances in safflower flowers and their applicability in medicine and health-promoting foods, *Int. J. Food Sci.* 2021 (2021), <https://doi.org/10.1155/2021/6657639>.
- [17] T. Bacchetti, C. Morresi, L. Bellachioma, G. Ferretti, Antioxidant and pro-oxidant properties of *Carthamus tinctorius*, hydroxy safflor yellow A, and safflor yellow A, *Antioxidants* 9 (2020), <https://doi.org/10.3390/antiox9020119>.
- [18] K. Alizadeh Yeloojeh, G. Saeidi, M.R. Sabzalian, Drought stress improves the composition of secondary metabolites in safflower flower at the expense of reduction in seed yield and oil content, *Ind. Crop. Prod.* 154 (2020), 112496, <https://doi.org/10.1016/j.indcrop.2020.112496>.
- [19] Y.L. Jun, J.C. Eun, J.K. Hyo, H.P. Jun, W.C. Sang, Antioxidative flavonoids from leaves of *Carthamus tinctorius*, *Arch. Pharm. Res.* 25 (2002) 313–319, <https://doi.org/10.1007/bf02976632>.
- [20] J. Asgarpanah, N. Kazemivash, Phytochemistry, pharmacology and medicinal properties of *Carthamus tinctorius* L, *Chin. J. Integr. Med.* 19 (2013) 153–159, <https://doi.org/10.1007/s11655-013-1354-5>.
- [21] A.D. Permana, I.A. Tekko, M.T.C. McCrudden, Q.K. Anjani, D. Ramadon, H. O. McCarthy, R.F. Donnelly, Solid lipid nanoparticle-based dissolving microneedles: a promising intradermal lymph targeting drug delivery system with potential for enhanced treatment of lymphatic filariasis, *J. Control. Release* 316 (2019) 34–52.
- [22] M.D. Triplett, J.F. Rathman, Optimization of β -carotene loaded solid lipid nanoparticles preparation using a high shear homogenization technique, *J. Nanopart. Res.* 11 (2009) 601–614, <https://doi.org/10.1007/s11051-008-9402-3>.
- [23] A. Zur Mühlen, C. Schwarz, W. Mehnert, Solid lipid nanoparticles (SLN) for controlled drug delivery - drug release and release mechanism, *Eur. J. Pharm. Biopharm.* 45 (1998) 149–155.
- [24] M.M. Mojahedian, S. Daneshamouz, S.M. Samani, A. Zargarani, A novel method to produce solid lipid nanoparticles using *n*-butanol as an additional co-surfactant according to the *o/w* microemulsion quenching technique, *Chem. Phys. Lipids* 174 (2013) 32–38, <https://doi.org/10.1016/j.chemphyslip.2013.05.001>.
- [25] M.B. McGuckin, J. Wang, R. Ghanma, N. Qin, S.D. Palma, R.F. Donnelly, A. J. Paredes, Nanocrystals as a master key to deliver hydrophobic drugs via multiple administration routes, *J. Control. Release* 345 (2022) 334–353, <https://doi.org/10.1016/j.jconrel.2022.03.012>.
- [26] T. Wang, J. Xue, Q. Hu, M. Zhou, Y. Luo, Preparation of lipid nanoparticles with high loading capacity and exceptional gastrointestinal stability for potential oral delivery applications, *J. Colloid Interface Sci.* 507 (2017) 119–130, <https://doi.org/10.1016/j.jcis.2017.07.090>.
- [27] E. Zimmermann, R.H. Müller, Electrolyte- and pH-stabilities of aqueous solid lipid nanoparticle (SLN) dispersions in artificial gastrointestinal media, *Eur. J. Pharm. Biopharm.* 52 (2001) 203–210, [https://doi.org/10.1016/S0939-6411\(01\)00167-9](https://doi.org/10.1016/S0939-6411(01)00167-9).
- [28] S. Qiu, D. Liang, F. Guo, T. Deng, T. Peng, Y. Gao, X. Zhang, H. Zhong, Solid lipid nanoparticles modified with amphipathic chitosan derivatives for improved stability in the gastrointestinal tract, *J. Drug Deliv. Sci. Technol.* 48 (2018) 288–299, <https://doi.org/10.1016/j.jddst.2018.10.007>.
- [29] S. Parvez, A. Karole, S.L. Mudavath, Transport mechanism of hydroxy-propyl-beta-cyclodextrin modified solid lipid nanoparticles across human epithelial cells for the oral absorption of antileishmanial drugs, *Biochim. Biophys. Acta - Gen. Subj.* 1866 (2022), 130157, <https://doi.org/10.1016/j.bbagen.2022.130157>.
- [30] J.S. Baek, J.W. So, S.C. Shin, C.W. Cho, Solid lipid nanoparticles of paclitaxel strengthened by hydroxypropyl- β -cyclodextrin as an oral delivery system, *Int. J. Mol. Med.* 30 (2012) 953–959, <https://doi.org/10.3892/ijmm.2012.1086>.
- [31] N.R. Naveen, C. Gopinath, D.S. Rao, Design expert supported mathematical optimization of repaglinide gastroretentive floating tablets: in vitro and in vivo evaluation, *Future J. Pharm. Sci.* 3 (2017) 140–147, <https://doi.org/10.1016/j.fjps.2017.05.003>.
- [32] H. Kathalia, S. Salunkhe, S. Juvekar, Formulation of gastroretentive sustained release floating in situ gelling drug delivery system of solubility enhanced curcumin-soy lecithin complex, *J. Drug Deliv. Sci. Technol.* (2019), <https://doi.org/10.1016/j.jddst.2019.101205>.
- [33] M. Rahamathulla, S. Saisivam, H.V. Gangadharappa, Development of valsartan floating matrix tablets using low density polypropylene foam powder: in vitro and in vivo evaluation, *AAPS PharmSciTech* 20 (2019) 1–10, <https://doi.org/10.1208/s12249-018-1265-z>.
- [34] S. Prasanthi, M. Vidyavathi, Formulation and optimization of buoyant in situ gelling system of valsartan using natural polymer, *Int. J. Pharm. Pharm. Sci.* 9 (2017) 128, <https://doi.org/10.22159/ijpps.2017v9i10.20809>.
- [35] L.M. Thomas, Formulation and evaluation of floating oral in-situ gel of metronidazole, *Int. J. Pharm. Pharm. Sci.* 6 (2014) 1–5.
- [36] A.Q. Vo, X. Feng, M. Pimparade, X. Ye, D.W. Kim, S.T. Martin, M.A. Repka, Dual-mechanism gastroretentive drug delivery system loaded with an amorphous solid dispersion prepared by hot-melt extrusion, *Eur. J. Pharm. Sci.* 102 (2017) 71–84, <https://doi.org/10.1016/j.ejps.2017.02.040>.
- [37] A. Himawan, N.J.N. Djide, S.A. Mardikasari, R.N. Utami, A. Arjuna, R.F. Donnelly, A.D. Permana, A novel in vitro approach to investigate the effect of food intake on release profile of valsartan in solid dispersion-floating gel in-situ delivery system, *Eur. J. Pharm. Sci.* 168 (2022), 106057, <https://doi.org/10.1016/j.ejps.2021.106057>.
- [38] M. Jafar, M. Salahuddin, S.R. Bolla, Gastric floating in-situ gel as a strategy for improving anti-inflammatory activity of meloxicam, *J. Appl. Pharm. Sci.* (2018), <https://doi.org/10.7324/JAPS.2018.81114>.
- [39] P.S. Rajinikanth, B. Mishra, Floating in situ gelling system for stomach site-specific delivery of clarithromycin to eradicate *H. pylori*, *J. Control. Release* (2008), <https://doi.org/10.1016/j.jconrel.2007.07.011>.
- [40] N.A.H. Abou Youssef, A.A. Kassem, M.A.E. El-Massik, N.A. Boraie, Development of gastroretentive metronidazole floating raft system for targeting *Helicobacter pylori*, *Int. J. Pharm.* 486 (2015) 297–305, <https://doi.org/10.1016/j.ijpharm.2015.04.004>.
- [41] D. Gadhave, N. Rasal, R. Sonawane, M. Sekar, C. Kokare, Nose-to-brain delivery of flutunomide-loaded lipid-based carbopol-gellan gum nanogel for glioma: pharmacological and in vitro cytotoxicity studies, *Int. J. Biol. Macromol.* 167 (2021) 906–920, <https://doi.org/10.1016/j.ijbiomac.2020.11.047>.
- [42] Y. Wang, P. Chen, C. Tang, Y. Wang, Y. Li, H. Zhang, Antinociceptive and anti-inflammatory activities of extract and two isolated flavonoids of *Carthamus tinctorius* L, *J. Ethnopharmacol.* 151 (2014) 944–950, <https://doi.org/10.1016/j.jep.2013.12.003>.
- [43] A.D. Permana, R.N. Utami, A.J. Courtenay, M.A. Manggau, R.F. Donnelly, L. Rahman, Phytosomal nanocarriers as platforms for improved delivery of natural antioxidant and photoprotective compounds in propolis: an approach for enhanced both dissolution behaviour in biorelevant media and skin retention profiles, *J. Photochem. Photobiol. B Biol.* 205 (2020), 111846.
- [44] A.D. Permana, Q.K. Anjani, E. Sartini, F. Utomo, A.J. Volpe-Zanutto, Y.M. Paredes, S.A. Evary, M.R. Mardikasari, I.N. Pratama, R.F. Donnelly Tuany, Selective delivery of silver nanoparticles for improved treatment of biofilm skin infection using bacteria-responsive microparticles loaded into dissolving microneedles, *Mater. Sci. Eng. C* 120 (2021), 111786.
- [45] A.D. Permana, A.J. Paredes, F. Volpe-Zanutto, Q.K. Anjani, E. Utomo, R. F. Donnelly, Dissolving microneedle-mediated dermal delivery of itraconazole nanocrystals for improved treatment of cutaneous candidiasis, *Eur. J. Pharm. Biopharm.* 154 (2020) 50–61, <https://doi.org/10.1016/j.ejpb.2020.06.025>.
- [46] A.D. Permana, A.J. Paredes, F.V. Zanutto, M.N. Amir, I. Ismail, M.A. Bahar, S. D. Sumarheni, R.F. Donnelly Palma, Albendazole nanocrystal-based dissolving microneedles with improved pharmacokinetic performance for enhanced treatment of cystic echinococcosis, *ACS Appl. Mater. Interfaces* 13 (2021) 38745–38760, <https://doi.org/10.1021/acsmi.1c11179>.
- [47] P.W.R. Ananda, D. Elim, H.S. Zaman, W. Muslimin, M.G.R. Tunggeng, A. D. Permana, Combination of transdermal patches and solid microneedles for improved transdermal delivery of primaquine, *Int. J. Pharm.* 609 (2021), 121204, <https://doi.org/10.1016/j.ijpharm.2021.121204>.
- [48] H.A. Qonita, N. Syafika, V. Valensie, J. Kamba, A. Maulana, A.D. Permana, Development water in oil nanoemulsion of diethylcarbamazine for enhanced the characteristics for lymphatic targeting: a proof of concept study, *J. Indian Chem. Soc.* 99 (2022), 100395, <https://doi.org/10.1016/j.jics.2022.100395>.
- [49] C.K. Enggi, H.T. Isa, S. Sulistiawati, K.A.R. Ardika, S. Wijaya, R.M. Asri, S. A. Mardikasari, R.F. Donnelly, A.D. Permana, Development of thermosensitive and

- mucoadhesive gels of cabotegravir for enhanced permeation and retention profiles in vaginal tissue: a proof of concept study, *Int. J. Pharm.* 609 (2021), 121182, <https://doi.org/10.1016/j.ijpharm.2021.121182>.
- [50] M. Mir, A.D. Permana, N. Ahmed, G.M. Khan, A. ur Rehman, R.F. Donnelly, Enhancement in site-specific delivery of carvacrol for potential treatment of infected wounds using infection responsive nanoparticles loaded into dissolving microneedles: a proof of concept study, *Eur. J. Pharm. Biopharm.* 147 (2020) 57–68.
- [51] D.J. Singhavi, R.S. Pundkar, S. Khan, Famotidine microspheres reconstituted with floating in situ gel for stomach-specific delivery: preparation and characterization, *J. Drug Deliv. Sci. Technol.* 41 (2017) 251–259, <https://doi.org/10.1016/j.jddst.2017.07.017>.
- [52] O.M. Kolawole, W.M. Lau, V.V. Khutoryanskiy, Chitosan/ β -glycerophosphate in situ gelling mucoadhesive systems for intravesical delivery of mitomycin-C, *Int. J. Pharm.* X 1 (2019), 100007, <https://doi.org/10.1016/j.ijpx.2019.100007>.
- [53] Y. Tang, Y. Zhao, Y. Li, Y. Du, A thermosensitive chitosan/poly(vinyl alcohol) hydrogel containing nanoparticles for drug delivery, *Polym. Bull.* 64 (2010) 791–804, <https://doi.org/10.1007/s00289-009-0214-0>.
- [54] F. Baxeveanis, P. Zampini, J. Kuiper, N. Fotaki, Investigation of drug partition kinetics to fat in simulated fed state gastric conditions based on drug properties, *Eur. J. Pharm. Sci.* 146 (2020), 105263, <https://doi.org/10.1016/j.ejps.2020.105263>.
- [55] H. Vaghasiya, A. Kumar, K. Sawant, Development of solid lipid nanoparticles based controlled release system for topical delivery of terbinafine hydrochloride, *Eur. J. Pharm. Sci.* 49 (2013) 311–322.
- [56] S. Das, W.K. Ng, R.B.H. Tan, Are nanostructured lipid carriers (NLCs) better than solid lipid nanoparticles (SLNs): development, characterizations and comparative evaluations of clotrimazole-loaded SLNs and NLCs? *Eur. J. Pharm. Sci.* 47 (2012) 139–151.
- [57] Q.K. Anjani, J. Domínguez-Robles, E. Utomo, M. Font, M.C. Martínez-Ohárriz, A. D. Permana, Á. Cárcamo-Martínez, E. Larraneta, R.F. Donnelly, Inclusion complexes of rifampicin with native and derivatized cyclodextrins: in silico modeling, formulation, and characterization, *Pharmaceuticals* 15 (2022), <https://doi.org/10.3390/ph15010020>.
- [58] H.T.H. Vu, S.M. Hook, S.D. Siqueira, A. Müllertz, T. Rades, A. McDowell, Are phytosomes a superior nanodelivery system for the antioxidant rutin? *Int. J. Pharm.* 548 (2018) 82–91.
- [59] B. Van Eerdenbrugh, G. Van den Mooter, P. Augustijns, Top-down production of drug nanocrystals: nanosuspension stabilization, miniaturization and transformation into solid products, *Int. J. Pharm.* 364 (2008) 64–75.
- [60] G.V. Patel, V.B. Patel, A. Pathak, S.J. Rajput, Nanosuspension of efavirenz for improved oral bioavailability: formulation optimization, in vitro, in situ and in vivo evaluation, *Drug Dev. Ind. Pharm.* 40 (2014) 80–91.
- [61] S. Das, W.K. Ng, R.B.H. Tan, Are nanostructured lipid carriers (NLCs) better than solid lipid nanoparticles (SLNs): development, characterisations and comparative evaluations of clotrimazole loaded SLNs and NLCs? *Eur. J. Pharm. Sci.* 47 (2012) 139–151, <https://doi.org/10.1016/j.ejps.2012.05.010>.
- [62] A.D. Permana, M.T.C. McCrudden, R.F. Donnelly, Enhanced intradermal delivery of nanosuspensions of antifilaria drugs using dissolving microneedles: a proof of concept study, *Pharmaceutics* 11 (2019) 346.
- [63] S. Zaki, H. Rizvi, F.A. Shah, N. Khan, I. Muhammad, K.H. Ali, M.M. Ansari, F. Din, O. Salman, K. Kim, Y. Choe, J. Kim, A. Zeb, Simvastatin-loaded solid lipid nanoparticles for enhanced anti-hyperlipidemic activity in hyperlipidemia animal model a Riphah, *Int. J. Pharm.* 560 (2019) 136–143.
- [64] M.N. Karemore, J.G. Avari, In-situ gel of nifedipine for preeclampsia: optimization, in-vitro and in-vivo evaluation, *J. Drug Deliv. Sci. Technol.* 50 (2019) 78–89, <https://doi.org/10.1016/j.jddst.2019.01.025>.
- [65] A.D. Permana, R. Nurul, P. Layadi, A. Himawan, N. Juniarti, Q. Kurnia, E. Utomo, S. Aulia, A. Arjuna, R.F. Donnelly, Thermosensitive and mucoadhesive in situ ocular gel for effective local delivery and antifungal activity of itraconazole nanocrystal in the treatment of fungal keratitis, *Int. J. Pharm.* 602 (2021), 120623.
- [66] A.D. Permana, E. Utomo, M.R. Pratama, M.N. Amir, Q.K. Anjani, S.A. Mardikasari, S. Sumarheni, A. Himawan, A. Arjuna, U. Usmanengsi, R.F. Donnelly, Bioadhesive-thermosensitive in situ vaginal gel of the gel flake-solid dispersion of itraconazole for enhanced antifungal activity in the treatment of vaginal candidiasis, *ACS Appl. Mater. Interfaces* 13 (2021) 18128–18141, <https://doi.org/10.1021/acsami.1c03422>.
- [67] D.B.E.D. Mahmoud, S. Marzok, In situ supersaturable polyhydrogels: a feasible modification of the conventional hydrogels for the enhanced delivery of stomach specific hydrophobic drugs, *J. Drug Deliv. Sci. Technol.* 58 (2020), 101744, <https://doi.org/10.1016/j.jddst.2020.101744>.
- [68] D.B. Mahmoud, M.H. Shukr, A.N. ElMeshad, Gastroretentive cosolvent-based in situ gel as a promising approach for simultaneous extended delivery and enhanced bioavailability of mitoglinide calcium, *J. Pharm. Sci.* 108 (2019) 897–906, <https://doi.org/10.1016/j.xphs.2018.09.020>.
- [69] M.N. Hsu, R. Luo, K.Z. Kwek, Y.C. Por, Y. Zhang, C.H. Chen, Sustained release of hydrophobic drugs by the microfluidic assembly of multistage microgel/poly (lactic-co-glycolic acid) nanoparticle composites, *Biomicrofluidics* 9 (2015) 1–7, <https://doi.org/10.1063/1.4916230>.